Universidade Federal de Goiás
Instituto de Física
Programa de Pós-Graduação em Física

Aryadine Fernandes de Sousa

Entropy Production in Quantum Systems and Nernst Heat Theorem for a Single Qubit

Goiânia
2024

UNIVERSIDADE FEDERAL DE GOIÁS
INSTITUTO DE FÍSICA

TERMO DE CIÊNCIA E DE AUTORIZAÇÃO (TECA) PARA DISPONIBILIZAR VERSÕES ELETRÔNICAS DE TESES

E DISSERTAÇÕES NA BIBLIOTECA DIGITAL DA UFG

Na qualidade de titular dos direitos de autor, autorizo a Universidade Federal de Goiás (UFG) a disponibilizar, gratuitamente, por meio da Biblioteca Digital de Teses e Dissertações (BDTD/UFG), regulamentada pela Resolução CEPEC nº 832/2007, sem ressarcimento dos direitos autorais, de acordo com a Lei 9.610/98, o documento conforme permissões assinaladas abaixo, para fins de leitura, impressão e/ou download, a título de divulgação da produção científica brasileira, a partir desta data.

O conteúdo das Teses e Dissertações disponibilizado na BDTD/UFG é de responsabilidade exclusiva do autor. Ao encaminhar o produto final, o autor(a) e o(a) orientador(a) firmam o compromisso de que o trabalho não contém nenhuma violação de quaisquer direitos autorais ou outro direito de terceiros.

1. Identificação do material bibliográfico

[X] Dissertação [ ] Tese [ ] Outro*:_____

*No caso de mestrado/doutorado profissional, indique o formato do Trabalho de Conclusão de Curso, permitido no documento de área, correspondente ao programa de pós-graduação, orientado pela legislação vigente da CAPES.

Exemplos: Estudo de caso ou Revisão sistemática ou outros formatos.

2. Nome completo do autor

Aryadine Fernandes de Sousa

3. Título do trabalho

Entropy production in quantum systems and Nernst heat theorem for a single qubit

4. Informações de acesso ao documento (este campo deve ser preenchido pelo orientador)

Concorda com a liberação total do documento [X] SIM [ ] NÃO[1]

[1] Neste caso o documento será embargado por até um ano a partir da data de defesa. Após esse período, a possível disponibilização ocorrerá apenas mediante:
a) consulta ao(à) autor(a) e ao(à) orientador(a);
b) novo Termo de Ciência e de Autorização (TECA) assinado e inserido no arquivo da tese ou dissertação.
O documento não será disponibilizado durante o período de embargo.
Casos de embargo:
- Solicitação de registro de patente;
- Submissão de artigo em revista científica;
- Publicação como capítulo de livro;
- Publicação da dissertação/tese em livro.

Obs. Este termo deverá ser assinado no SEI pelo orientador e pelo autor.

Documento assinado eletronicamente por **Norton Gomes De Almeida**, **Professor do Magistério Superior**, em 29/02/2024, às 15:30, conforme horário oficial de Brasília, com fundamento no § 3º do art. 4º do Decreto nº 10.543, de 13 de novembro de 2020 .

Documento assinado eletronicamente por **Aryadine Fernandes De Sousa**, **Discente**, em 29/02/2024, às 15:35, conforme horário oficial de Brasília, com fundamento no § 3º do art. 4º do Decreto nº 10.543, de 13 de novembro de 2020.

A autenticidade deste documento pode ser conferida no site https://sei.ufg.br/sei/controlador_externo.php?acao=documento_conferir&id_orgao_acesso_externo=0, informando o código verificador **4417606** e o código CRC **B0FF864D**.

Referência: Processo nº 23070.008010/2024-41 SEI nº 4417606

Aryadine Fernandes de Sousa

Entropy Production in Quantum Systems and Nernst Heat Theorem for a Single Qubit

Produção de Entropia em Sistemas Quânticos e o Teorema do Calor de Nernst para um Único Qubit

Dissertation defended in the Postgraduate Program of Physics at the Physics Institute at the Federal University of Goiás as the final requirement for the Master's degree in Physics.

Concentration Area: Physics

Research Line: Quantum Optics and Quantum Information

Advisor: Prof. Dr. Norton Gomes de Almeida

Goiânia
2024

Ficha de identificação da obra elaborada pelo autor, através do
Programa de Geração Automática do Sistema de Bibliotecas da UFG.

Sousa, Aryadine Fernandes de
Entropy Production in Quantum Systems and Nernst Heat Theorem for a Single Qubit [manuscrito] / Aryadine Fernandes de Sousa. - 2024.
78 f.: il.

Orientador: Prof. Dr. Norton Gomes de Almeida.
Dissertação (Mestrado) - Universidade Federal de Goiás, Instituto de Física (IF), Programa de Pós-Graduação em Física, Goiânia, 2024.
Bibliografia. Apêndice.

1. Quantum Thermodynamics. 2. Entropy Production. 3. Heat Engines. 4. Heat Engines. 5. Nernst Heat Theorem. I. Almeida, Norton Gomes de, orient. II. Título.

CDU 53

UNIVERSIDADE FEDERAL DE GOIÁS

INSTITUTO DE FÍSICA

ATA DE DEFESA DE DISSERTAÇÃO

Ata nº 216 da sessão de Defesa de Dissertação de Aryadine Fernandes de Sousa, que confere o título de Mestra em Física, na área de concentração em Física.

Aos 23 dias do mês de fevereiro de 2024, a partir das 08h30min, por meio de videoconferência, realizou-se a sessão pública de Defesa de Dissertação intitulada “Entropy production in quantum systems and Nernst heat theorem for a single qubit”. Os trabalhos foram instalados pelo Orientador, Professor Doutor Norton Gomes de Almeida (IF/UFG), com a participação dos demais membros da Banca Examinadora: Professor Doutor Alexandre Martins de Souza (CBPF), membro titular externo; e Professor Doutor Gentil Dias de Moraes Neto (Zhejiang Normal University / China), membro titular externo. Durante a arguição, os membros da banca não fizeram sugestão de alteração do título do trabalho. A Banca Examinadora reuniu-se em sessão secreta a fim de concluir o julgamento da Dissertação, tendo sido a candidata aprovada pelos seus membros. Proclamados os resultados pelo Professor Doutor Norton Gomes de Almeida, Presidente da Banca Examinadora, foram encerrados os trabalhos e, para constar, lavrou-se a presente ata que é assinada pelos membros da Banca Examinadora, aos 23 dias do mês de fevereiro de 2024.

TÍTULO SUGERIDO PELA BANCA

Documento assinado eletronicamente por **Alexandre Martins de Souza**, **Usuário Externo**, em 23/02/2024, às 10:17, conforme horário oficial de Brasília, com fundamento no § 3º do art. 4º do Decreto nº 10.543, de 13 de novembro de 2020 .

Documento assinado eletronicamente por **GENTIL DIAS DE MORAES NETO**, **Usuário Externo**, em 23/02/2024, às 10:18, conforme horário oficial de Brasília, com fundamento no § 3º do art. 4º do Decreto nº 10.543, de 13 de novembro de 2020 .

Documento assinado eletronicamente por **Norton Gomes De Almeida**, **Professor do Magistério Superior**, em 23/02/2024, às 10:18, conforme horário oficial de Brasília, com fundamento no § 3º do art. 4º do Decreto nº 10.543, de 13 de novembro de 2020 .

A autenticidade deste documento pode ser conferida no site https://sei.ufg.br/sei/controlador_externo.php?acao=documento_conferir&id_orgao_acesso_externo=0, informando o código verificador **4379555** e o código CRC **C065AFC3**.

Referência: Processo nº 23070.008010/2024-41 SEI nº 4379555

To my mother, my father and my sister.

Acknowledgments

I would like to express my deep gratitude to everyone who played crucial roles in the completion of this dissertation.

First and foremost, to my family and my roommate Pedro Ivo, whose constant support and understanding were the anchor that sustained me throughout this academic journey. I am profoundly grateful to those who were not only an inspiration but also a safe harbor - Laryssa Ferro, Lucas Aurélio, and Ardiley Torres.

To the friends from room 215, Gustavo Oliveira, Henrique Chagas, and Igor Froldi, and to Thiago Moreira, who, even though not officially part of the room, shared unforgettable moments with me. Sharing the room with all of you was one of the best choices I made during this journey.

To friends Bruno Miranda, Pedro Bento, and Rodrigo Amorim, who marked my path in post-graduation. A special thanks to Gabriella Damas, whose support goes beyond the colleague relationship in the research group; her friendship and support were invaluable. I cannot forget to thank friends Fabio Vaz, Juracy Leandro, and Pedro Augusto Aquino for the moments of relaxation and wonderful conversations that were essential.

To my advisor, Norton Gomes de Almeida, who has been with me from undergraduate studies to this moment. His guidance, wisdom, and support were crucial for the development of this work and for my professional growth. To collaborating researchers Rogerio Assis, Carlos Henrique, Roberto Serra, and Celso Villas Boas, my sincere thanks for their valuable contribution and exchange of knowledge.

Finally, I thank the Institute of Physics at the Federal University of Goiás and the funding agencies CAPES and CNPq for making this work possible.

This book was written by a woman who climbed the Mountain of Life by removing stones and planting flowers.

– Cora Coralina

Resumo

A termodinâmica clássica fundamenta-se na análise de sistemas macroscópicos em equilíbrio, originando diversas teorias para abordar sistemas fora de equilíbrio ao longo do tempo. Recentemente, a termodinâmica quântica emergiu como uma teoria especializada na descrição de sistemas quânticos microscópicos. Um exemplo notável dessa teoria é observado no desenvolvimento de motores térmicos, nos quais a substância funcional é um sistema quântico em escala microscópica.

Neste trabalho apresentamos a formulação teórica essencial para compreender a produção de entropia em sistemas quânticos e seu impacto em máquinas térmicas. A abordagem envolve explorar o atrito quântico e conduzir uma análise mais profunda das leis da termodinâmica em escala fundamental.

Ao examinar os efeitos desses fenômenos em um Ciclo de Otto Quântico, destacamos as implicações do atrito quântico no desempenho do motor. Notavelmente, observamos que operar o ciclo com um reservatório de temperatura negativa efetiva resulta em um aumento significativo na eficiência do motor. Em nossa pesquisa, demonstramos que essa melhoria decorre de escolhas estratégicas nas populações de estados excitados nos reservatórios, revelando uma abordagem para otimizar o desempenho em para esses motores quânticos.

Além disso, estendemos o teorema do calor de Nernst para um único qubit. Este resultado não só apresenta implicações teóricas intrigantes, mas também é apoiado por simulações numéricas e experimentos utilizando Ressonância Magnética Nuclear (RMN). Essas evidências sustentam a convergência da energia livre de Helmholtz e da energia interna à medida que a temperatura se aproxima de zero Kelvin, demonstrando uma extensão deste teorema em sistemas quânticos.

Palavras - chave: Termodinâmica Quântica, Produção de Entropia, Motores Térmicos, Fricção Quântica, Teorema do Calor de Nernst.

Abstract

Classical thermodynamics, which focuses on macroscopic systems in equilibrium, has given rise to various theories to address systems out of equilibrium over time. Recently, quantum thermodynamics has emerged as a theory dedicated to describe microscopic quantum systems. A notable application of this theory is found in the development of thermal engines, where the working substance is a microscopic quantum system.

In this work, we present the essential theoretical formulation to understand entropy production in quantum systems and its impact on thermal machines. The approach involves exploring quantum friction and conducting a deeper analysis of the laws of thermodynamics on a fundamental scale.

Examining the effects of these phenomena in a Quantum Otto Heat Engine, we highlight the implications of quantum friction on engine performance. Particularly noteworthy is the observation that operating the cycle with a reservoir with effective negative temperature enhances the engine efficiency significantly. This improvement is attributed to strategic choices in the populations of excited states in the reservoirs, revealing an innovative approach to optimizing performance in quantum systems.

Additionally, we extend the Nernst heat theorem for a single qubit. This result not only presents intriguing theoretical implications but is also supported by numerical simulations and experiments using Nuclear Magnetic Resonance (NMR). These pieces of evidence uphold the remarkable convergence of Helmholtz free energy and internal energy as the temperature approaches zero Kelvin, underscoring the practical applicability of these theorems in quantum systems.

Key - words: Quantum Thermodynamics, Entropy Production, Heat Engines, Quantum Friction, Nernst Heat Theorem.

List of Figures

List of Acronyms

QOHE Quantum Otto Heat Engine

TLS Two-Level System

NMR Nuclear Magnetic Resonance

Contents

CHAPTER 1

Introduction

The understanding the processes related to heat, energy and their transformations constituted the main impulse for the development of Thermodynamic. The interaction between heat and matter has been acknowledged since antiquity, although lacking a formal understanding .

In the 17th century, Galileo Galilei inaugurated investigations into heat, although in the absence of an established theoretical basis [4]. The advent of the industrial revolution intensified the need to understand the conversion of thermal energy into mechanical energy. In 1824, Sadi Carnot established the theoretical foundations governing the efficiency of ideal heat engines [4]. Throughout the 20th century, Classical Thermodynamics found multiple applications and expanded its scope, interconnecting, for example, with information theory through the Landauer principle, thus establishing such a connection. The phenomenological approach adopted by Thermodynamics focuses on the description and prediction of macroscopically observable phenomena, refraining from delving into explanations at the microscopic level. Quantum Thermodynamics arises with the challenge of extending the principles of thermodynamics to microscopic systems [5], where the definitions between work and heat are not as clear as in macroscopic cases.

In both classical and quantum thermodynamics, irreversibility, which emerges from the entropy production, is an indispensable topic when the objective is to understand how heat engines work, as it determines the amount of useful energy obtained in a given process. Due to such importance, this work aims to analyze different contexts in which entropy production occurs in quantum systems.

The entropy production results in the loss of part of the energy that could be used to perform work [6]. We will call this portion of irreversible work, which can be classified in two ways in quantum systems. The first is quantum friction, related to transitions between states when executing a protocol that transforms the Hamiltonian in finite times. The second form is called residual lag, associated with the entropy production during the thermalization process.

In addition to the entropy production, another subject of interest to us is understanding how classical laws extend to quantum systems, especially the third law. This law addresses relevant issues, such as limits for thermometry [7], scalability and initialization of quantum computer records in pure states [8], realization of ideal projective measurements [9], among others.

In the second chapter, we review the basic concepts of classical thermodynamics, delving deeper into topics such as laws and heat engines. We will emphasize the third law, as it is in our interest to carry out a more in-depth analysis of this in quantum systems.

In the third chapter, we present the fundamental principles of quantum thermodynamics. Our exploration covers topics including open quantum systems, the application of thermodynamic laws in this context, the dynamics of systems involving reservoirs with negative effective temperatures. Still in this same chapter, delving deeper into the domain of quantum thermodynamics, we examine the relationship between the cooling rate and the third laws of thermodynamics. We also examine the emergence of irreversibility in these systems through the Tasaki-Crooks theorem, establishing a link between this irreversibility and quantum friction. Finally, we present the Quantum Otto Heat Engine (QOHE) with an interest in the impact of entropy production in this cycle.

In the fourth chapter, we present our results, demonstrating that, for a Quantum Otto Engine with one of the reservoirs with a negative effective temperature, friction work can improve engine performance. As a result, we observed significant gains in engine efficiency and power [10]. In this same chapter, we show in an unprecedented way the result of Nernst Heat Theorem and The Unattainability Principle for a single qubit with experimental results using the technique of Nuclear Magnetic Resonance (NMR) [11]. To this end, it was necessary to find the analogous thermodynamic potentials for quantum systems. Finally, in the fifth chapter, we present the conclusions and offer perspectives regarding this study.

CHAPTER 2

Concepts in Classical Thermodynamics

Classical thermodynamics originates entirely from a phenomenological point of view, and questions concerning the nature of heat and the mechanisms of its transfer from one body to another persisted without definitive answers from antiquity until the 20th century [4]. In this chapter, we present some of the mathematical tools necessary for this work. For this reason, we will focus our attention on a brief review of the fundamental concepts that form the basis of classical thermodynamics, providing an exposition of the laws that govern it, as well as heat engines. In addition, we will also introduce the concept of negative effective temperature.

2.1 Laws of Thermodynamics

The laws of thermodynamics provide a basis for understanding the interaction and transformation of energy in systems. They establish principles such as energy conservation and the irreversibility of natural processes, allowing predictions and optimizations in complex systems such as engines and chemical reactions.

The *Zero Law of Thermodynamics* establishes the basis for the definition of temperature, which is intrinsically related to the concept of thermal equilibrium. When we deal with closed systems, that is, systems that can exchange energy with the external environment, but do not allow the transfer of matter, it is possible to state that a system is in equilibrium when its state variables remain constant over a period long enough.

In this context, when two systems reach thermal equilibrium, they share an intensive property called temperature. This property does not depend on the amount of matter present in the systems. Thus, we can state the Zeroth Law of Thermodynamics as follows:

Given three systems, denoted A, B, and C, if systems A and B reach thermal equilibrium with each other, and systems B and C also reach thermal equilibrium with each other, then we can conclude that systems A and C are in thermal equilibrium with each other.

The next law is about conservation of energy, it is possible to associate an internal energy U to each macroscopic system. For an isolated system, that is, a system that does not exchange work or heat with the environment, the internal energy U coincides with the total energy E of the system, known from mechanics or electrodynamics. However, when a system has the capacity to exchange work or heat with the environment, the change in internal energy for an arbitrary change of state, whether reversible or irreversible, is determined by the sum of the work W and the heat Q. This principle is known as the *First Law of Thermodynamics* and can be summarized in the equation:

$$dU = \delta W + \delta Q. \tag{2.1}$$

The work and heat exchanged with the environment depend on how the process takes place, while the change in internal energy depends only on the initial and final states of the system. Therefore, internal energy is an exact differential, unlike heat and work. For this reason, we employ the symbol δ to differentiate these infinitesimals.

The Second Law can be presents in different ways. Concisely, we can express it through the Clausius and Kelvin-Planck Statements, which are the following:

Clausius Statements: *"It is not possible to transfer heat from a cold body to a hot body without performing work on the system."*

Kelvin-Planck Statements: *"It is impossible to build a heat engine that operates in cycle integrally converting heat into work, without the requirement to transfer heat to a lower temperature reservoir."*

The statements not only reveal the limitations of how heat engines operate but also establish restrictions on their performance. These restrictions were investigated by Carnot, and we will examine them in the next section. Clausius introduced a state function called entropy (S), which represents the amount of heat exchanged with the environment at temperature T in a reversible process (i.e., a process that occurs only between equilibrium states)

$$dS = \frac{\delta Q_{rev}}{T}. \tag{2.2}$$

Considering that the amount of heat δQ_{irr} exchanged in an irreversibly process is always less than that exchanged in a reversible process, δQ_{rev}, we can conclude that

$$\delta Q_{irr} < \delta Q_{rev}. \tag{2.3}$$

For an isolated system, with no exchange of matter or energy, this implies that

entropy remains constant at thermodynamic equilibrium and reaches its maximum value with $dS = 0$ [12]. However, all irreversible processes in an isolated system that lead to equilibrium are associated with an increase in entropy. These formulation of the *Second Law of Thermodynamics* can be resumed in the following Equation:

$$dS \geq 0, \tag{2.4}$$

the equality occur in the reversible processes.

The *Third Law of Thermodynamics*, in a more modern perspective, deals with the unattainability of absolute zero. One of the pioneering attempts to determine the value of this minimum temperature was carried out by Guillaume Amontons, who found an approximate value of -239^oC [13]. He based this estimate on observations made with an air thermometer he had developed himself. Later, absolute zero was established as 0 Kelvin (0 K), which corresponds to -273 degrees Celsius [12].

Initially, the Third Law originated from Nernst's Postulate. In his quest to understand the behavior of entropy and energy at extremely low temperatures, he published "The New Theorem of Heat" in 1907 [14]. In this work, Nernst articulated:

"... in the neighbourhood of the absolute zero all processes proceed without alteration of entropy" [14].

Let there be a change in Gibbs potential

$$\Delta G = \Delta H - T\Delta S, \tag{2.5}$$

the changed of entropy

$$\Delta S = \frac{\Delta H - \Delta G}{T}, \tag{2.6}$$

to analyze the change of entropy at the limit of low temperatures, we have

$$\lim_{T\to 0} \Delta S = \lim_{T\to 0} \frac{\Delta H - \Delta G}{T}. \tag{2.7}$$

Note that this limit presents an indeterminacy that allows us to use L'Hôpital's rule. Thus, we can observe that the slopes of the tangent lines to the curves of Enthalpy and Gibbs energy variation are equal if the change in entropy is equal to zero, as shown in Figure 2.1a

$$\frac{\partial \Delta H}{\partial T} = \frac{\partial \Delta G}{\partial T}. \tag{2.8}$$

We can state that the change in enthalpy and Gibbs free energy of a system in equilibrium tend to the same value in the limit in which the temperature approaches absolute zero during an isothermal process. In other words, as $T \to 0$ is an isotherm it is also an adiabatic.

Nernst stated that these curves converged to the same value at low-temperature regimes, and the same holds true for internal energy and Helmholtz energy.

$$\lim_{T\to 0} \Delta S = \lim_{T\to 0} \frac{\Delta U - \Delta F}{T} \equiv 0, \tag{2.9}$$

$$\frac{\partial \Delta U}{\partial T} = \frac{\partial \Delta F}{\partial T}. \tag{2.10}$$

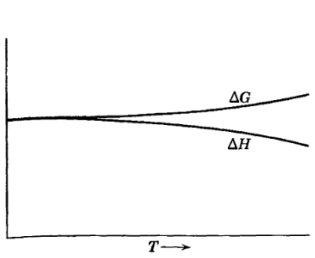

(a) Figure taken from [12].

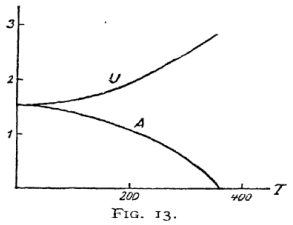

FIG. 13.

(b) Figure taken from [14].

Figure 2.1: Thermodynamics Potentials at limit of low temperatures.

The Nernst theorem has often been criticized for missing a demonstration based on thermodynamic principles [15]. In one of his numerous attempts to justify the theorem, Nernst also posits that the specific heat tends to zero at the low-temperature limit [15]

$$\lim_{T\to 0} C_V = \lim_{T\to 0} \left(\frac{\partial U}{\partial T}\right)_V = 0, \tag{2.11}$$

$$\lim_{T\to 0} C_P = \lim_{T\to 0} \left(\frac{\partial U}{\partial T}\right)_P = 0. \tag{2.12}$$

When considering that the specific heat tends to zero at the limit of low temperatures, it implies that the system's ability to absorb thermal energy becomes increasingly lower. As a result, an infinitely large amount of energy would be required to cause a temperature change in the system. Therefore, as a consequence of Nernst's postulate, it is affirmed that reaching absolute zero is not possible using only thermodynamic methods [12].

Planck also contributed to the third law, which is why it is known as the Nernst-Planck postulate. In 1910, Planck, for statistical considerations, postulated that the entropy of all perfect crystalline substances is the same at absolute zero and can be considered as zero [12]. This consideration is valid since, if we consider a system with a non-degenerate ground state, the number of ways in which all particles can be organized in that state is unique and, therefore, the entropy must be zero. This formulation is flawed when applied to glassy and amorphous substances, as they exhibit a residual entropy [16].

Albert Einstein was one of the harshest critics of Nernst's work [15], and his criticisms were considered valid, as there was no satisfactory demonstration of the

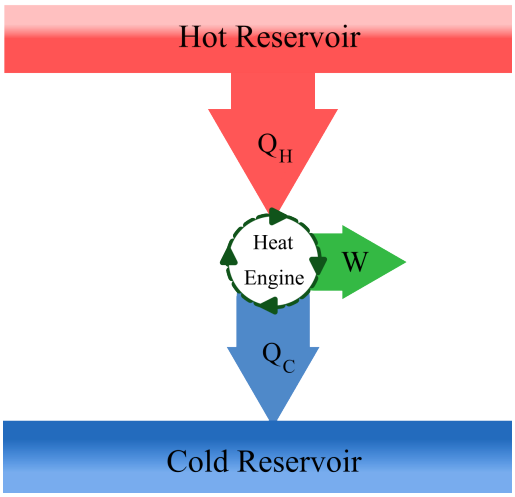

Figure 2.2: Schematic figure of the operation of a thermal machine. The red arrow denotes the energy $Q_H > 0$ absorbed by the system from the hot reservoir, the blue arrow signifies the energy $Q_C < 0$ expelled into the cold reservoir, and the green arrow illustrates the energy converted into useful work $W < 0$.

theorem or experimental confirmation up to that moment. Einstein argued that although the accurate prediction of the disappearance of specific heats makes the theorem more acceptable, this does not constitute evidence that it can be derived exclusively using the theory of classical thermodynamics.

In order to reinforce the idea that the heat theorem could be demonstrated only through thermodynamic arguments, without the need for quantum theory, Nernst developed a second argument based on the principle of unattainability [15].

2.2 Heat Engines

As previously mentioned, heat engines have been of paramount importance in the development of thermodynamics. For this reason, we will present here two thermal cycles: the Carnot cycle, which provides us with an important result regarding the efficiency limit of cyclic heat engines, and we will also address the Otto cycle, whose quantum aspect will be part of the results of this work.

The heat engines are devices designed to convert a portion of thermal energy (heat) into useful work. However, complete conversion of heat into work is not possible due to the second law of thermodynamics.

In this work we will interested on engines cyclic manner, absorbing a quantity of heat denoted as Q_H from a hot reservoir. A portion of this energy is then converted into work, represented as W, while the other part, Q_C, is dissipated to a cold reservoir. This process is illustrated schematically in the Figure 2.2.

With regard to the performance of these machines, we can calculate the efficiency and the power. Efficiency is defined as the ratio between the amount of work obtained

and the amount of heat absorbed.

$$\eta = \frac{-W}{Q_H}, \tag{2.13}$$

where the sign in the expression arises from the adoption of the convention that all energy leaving the system is considered negative, while all energy entering the system is considered positive. In this way, both the work done and the heat transferred Q_C have negative signs. Note that, in accordance with the Kelvin-Planck statement, the way efficiency has been defined implies that efficiency will always be less than one.

Power, in turn, is defined as the ratio between the work done and the cycle time τ

$$P = \frac{-W}{\tau}. \tag{2.14}$$

In the context of the efficiency of heat engines, we must highlight the Carnot cycle. This cycle defines the theoretical limits of efficiency that ideal thermal machines can achieve.

The Carnot cycle was developed by Sadi Carnot in 1824. It is a thermodynamic model that describes the behavior of a hypothetical thermal machine operating between two heat sources, one hot and the other cold. Its maximum theoretical efficiency serves as a point of reference for comparing the performance of other heat engines. The Carnot cycle consists of four reversible stages, which are: one isothermal volumetric expansion (at the constant temperature of the hot source), one adiabatic expansion (no heat exchange with the source), one isothermal compression (at the constant temperature of the cold source), and one adiabatic compression.

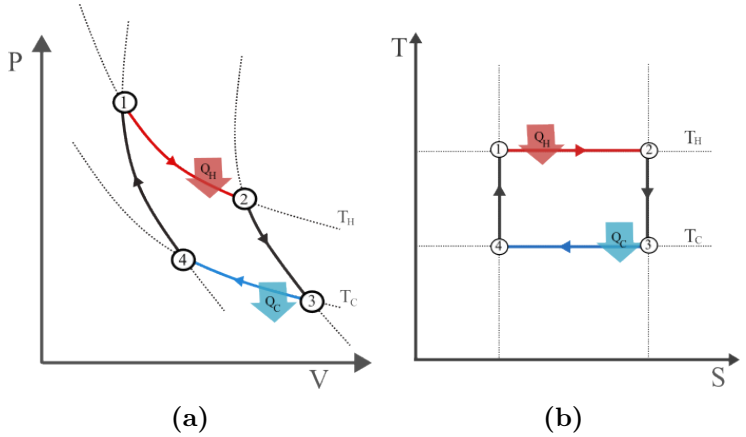

Figure 2.3: Schematic diagram of the operation of Carnot cycle (a)PV diagram (b)ST diagram.

The efficiency of the Carnot cycle is only determined by the temperatures of the heat sources and the relationship between the absolute temperatures of these sources. Taking into account the conservation of energy, imposed by the first law of thermodynamics, and the fact that, at the end of the cycle, the change in internal energy

is zero, we can express the work done as $W = |Q_C| - Q_H$. Substituting this into Equation 2.13, we obtain:

$$\eta = 1 - \frac{|Q_C|}{Q_H}, \tag{2.15}$$

as shown in the diagram, the change in entropy during adiabatic expansions and compressions is equal, as the cycle operates in reversible processes, we can take the integral of Equation 2.2 for the entire cycle and write

$$\frac{Q_H}{T_H} = \frac{|Q_C|}{T_C}. \tag{2.16}$$

In this cycle, the amount of heat corresponds to the ratio of temperatures, so:

$$\eta_{Carnot} = 1 - \frac{T_C}{T_H}. \tag{2.17}$$

This is the efficiency limit of a heat engine. Note that the efficiency is independent of the working substance used in the cycle, depending only on the temperatures of the reservoirs. Although the Carnot cycle is a theoretical ideal that cannot be achieved in practice due to losses and irreversibilities in real systems, it provides an important reference point for understanding the actual performance of thermal machines.

The Otto cycle operates on internal combustion and is the cycle that most closely resembles gasoline engines [12]. This cycle consists of the following stages: Adiabatic Compression ($1 \rightarrow 2$), Isochoric Heating ($2 \rightarrow 3$), Adiabatic Expansion ($3 \rightarrow 4$), and finally, it is cooled at constant volume ($4 \rightarrow 1$), as illustrated in the diagram.

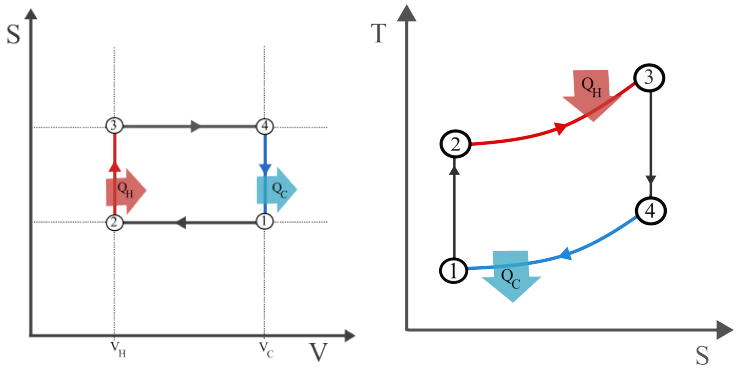

Figure 2.4: Schematic diagram of the operation of Otto cycle (a)SV diagram (b)ST diagram.

In contrast to the Carnot cycle, heat absorption in the idealized Otto cycle does not occur at a constant temperature. For the cycle to be reversible, during the expansion stage, the system passes through an infinite series of thermal reservoirs with gradual temperature variation. Each subsequent reservoir is infinitesimally larger than

the previous one. The final volume of the expansion is represented by V_H. Likewise, in the compression stage, the reservoirs have lower temperatures, and at the end of compression, the volume is V_C.

Assuming that the working substance is an ideal gas with heat capacities independent of temperature, we can calculate the efficiency for the Otto cycle as follows:

$$\eta_{Otto} = 1 - \left(\frac{V_C}{V_H}\right)^{\gamma-1}, \tag{2.18}$$

with γ representing the adiabatic expansion coefficient.

Consider now that the heat absorbed in the constant volume stage, represented by Q_H, and the heat given up, represented by Q_C, are given by

$$Q_H = c_V(T_3 - T_2), \tag{2.19}$$

$$Q_C = c_V(T_1 - T_4). \tag{2.20}$$

Let the efficiency be $\eta = 1 - |Q_C|/Q_H$, we then have

$$\eta = 1 - \frac{|T_1 - T_4|}{(T_3 - T_2)} = 1 - \frac{T_1}{T_2}\frac{(T_4/T_1 - 1)}{(T_3/T_2 - 1)}, \tag{2.21}$$

if $T_4/T_1 = T_3/T_2$ efficiency corresponds to

$$\eta = 1 - \frac{T_1}{T_2}. \tag{2.22}$$

Note that, given this condition, the efficiency of the Otto cycle can be expressed exclusively in terms of the temperature relationship, as well as the Carnot cycle.

2.3 Thermodynamic at Effective Negative Temperature

As previously highlighted, systems in thermal equilibrium share a common temperature. From a quantum perspective, we can observe that lower energy levels are more often occupied than higher levels. However, in situations of population inversion, in which higher energy levels become more populated than lower levels, a counter-intuitive characteristic emerges: the presence of a negative effective temperature in the system. In 1950, Edward Purcell introduced this concept by considering spin states with inverted populations and describing them as states characterized by negative spin temperatures [17].

Purcell and Pound [17] conducted an experiment with a nuclear spin system

in a lithium fluoride crystal, with the aim of identifying the conditions that lead to remagnetization. For a state of reverse magnetization to occur, there must be a population inversion, indicating that higher energy levels become more populated than lower ones.

With regard to thermodynamic quantities and the statistics that describe states with negative temperature values, Ramsey addressed this topic in his paper in 1956 [1]. He highlighted that entropy is not necessarily a monotonically increasing function of internal energy, and the behavior of entropy considering the case in which there is population inversion can be represented as:

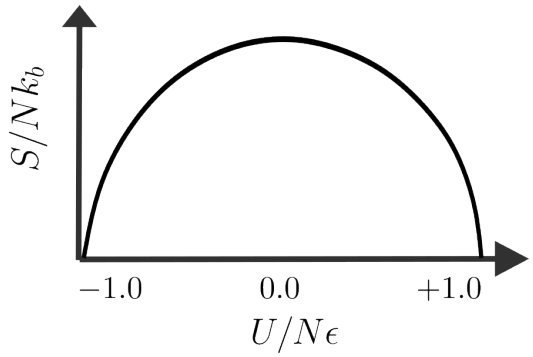

Figure 2.5: Entropy versus internal energy for a two-state system. The energy of the system is $\pm\epsilon$, and k_B is the Boltzmann constant. Schematic figure adapted from [1].

The maximum of the entropy curve, as shown in the previous figure, corresponds to $\partial U/\partial S = 0$ and, consequently, to the case in which the temperature is infinite. The range where $\partial U/\partial S < 0$ means negative effective temperature. For this reason, the negative temperature is seen as "hotter" than the infinite temperature, we can represent the scale from cold to hot according to:

$$+0\text{K}, \cdots, +300\text{K}, \cdots, +\infty\text{K}, -\infty\text{K}, \cdots, -300\text{K}, \cdots, -0\text{K}.$$

When revisiting the laws of thermodynamics under the consideration of negative effective temperature, we observe that the definitions of heat and work remain unchanged. Likewise, the first law maintains its consistency for both positive and negative temperatures [1]. The definitions of entropy and Clausius' statement also remain unchanged. However, to adjust the Kelvin-Planck statement to take into account the negative temperature case, modifications are necessary: creating a device in a closed system solely extracting heat from a positive temperature reservoir for work or rejecting heat into a negative-temperature reservoir, while work is done on the engine, is deemed impossible. Importantly, absolute zero temperature remains unattainable.

In the next few chapters, we will explore negative effective temperature, focusing exclusively on two-level systems. The focus will be on the efficiency of quantum thermal machines, particularly those in which one of the reservoirs has this property.

CHAPTER 3

Quantum Thermodynamics

Quantum Thermodynamics emerges as a recent area of study in physics with the purpose of deepening the understanding of thermodynamic principles in association with quantum phenomena. It is known that the quantum behavior of systems can be lost due to temperature, which motivates the need for investigations in this area.

In this chapter, we will explore concepts related to Quantum Thermodynamics, as well as its laws and the production of entropy. Additionally, we will discuss the application of these principles in the context of the Quantum Otto Heat Engine (QOHE).

3.1 The Gibbs State and Quantum Markovian Master Equation in Two-Level Systems

Open quantum systems are those that interact and exchange energy, matter or information with the surrounding environment. Unlike isolated systems, which have no interactions with the environment, open quantum systems are subject to external influences that can result in loss of energy, decoherence (loss of quantum coherence).

Within this context, a reservoir (R) is the environment that surrounds the system (S) and is in constant exchange of energy, matter or information. This reservoir can be of a thermal nature (involving exchanges of thermal energy), photonic (involving exchanges of light particles) or any other external nature.

Considering that the quantum system is in thermal equilibrium with the thermal reservoir, we can demonstrate that this equilibrium state, also known as the Gibbs state, is characterized by the maximum von Neumann entropy. To illustrate this, let's take an equilibrium state ρ_{eq} with a basis of states $|\lambda_i\rangle$. When $\rho_{th}|\lambda_i\rangle = p_i|\lambda_i\rangle$, the von Neumann entropy is maximized.

$$S_{vN} = -\sum_{i=1}^{n} \langle\lambda_i| \rho_{th} \ln \rho_{th} |\lambda_i\rangle = -\sum_{i=1}^{n} p_i \ln p_i. \tag{3.1}$$

We can maximize the entropy using Lagrange multipliers. Consider introducing Lagrange multipliers γ and β into the Lagrangian function:

$$s(p) = -\sum_{i=1}^{n} p_i \ln p_i + \gamma(\sum_{i=1}^{n} p_i - 1) + \beta\left(\langle H\rangle - \sum_{i=1}^{n} p_i E_i\right), \tag{3.2}$$

where $\langle H\rangle = \mathrm{Tr}\{\rho_{th}H\} = \sum_{i=1}^{n} p_i E_i = U = constant$, is the internal energy. We also consider $H\left|\lambda_i\right\rangle = E_i\left|\lambda_i\right\rangle$ and $\sum_{i=1}^{n} p_i = 1$. Taking the derivative of the function:

$$\frac{\partial s(p_i)}{\partial p_j} = \sum_{i=1}^{n}\left(-\delta_{ji}\ln pi - p_i\frac{1}{p_i}\delta_{ij} + \gamma\delta_{ij} - \beta\delta_{ij}E_i\right) = 0 \tag{3.3}$$

that means

$$-\ln p_i - 1 + \gamma - \beta E_i = 0. \tag{3.4}$$

Isolating p_i in this expression

$$p_i = e^{-1+\gamma-\beta E_i}, \tag{3.5}$$

considering that $\sum_i^n p_i = 1$ we have

$$e^{-1+\gamma}\sum_{i}^{n} e^{-\beta E_i} = 1, \tag{3.6}$$

$$e^{-1+\gamma} = \frac{1}{\sum_i^n e^{-\beta E_i}} \equiv \frac{1}{Z} \tag{3.7}$$

that implies

$$p_i = \frac{1}{Z}e^{-\beta E_i}, \tag{3.8}$$

The distribution is known as the Gibbs distribution. Assuming that ρ and H can be diagonalized in the same basis, and $[\rho_{th}, H] = 0$, we obtain

$$\rho_{th} = \sum_{i}^{n} p_i\left|\lambda_i\right\rangle\left\langle\lambda_i\right| = \sum_{i}^{n}\frac{1}{Z}e^{-\beta E_i}\left|\lambda_i\right\rangle\left\langle\lambda_i\right| = \sum_{i}^{n}\frac{1}{Z}e^{-\beta H}\left|\lambda_i\right\rangle\left\langle\lambda_i\right|. \tag{3.9}$$

Identify the completeness relation within it

$$\rho_{th} = \frac{e^{-\beta H}}{Z}, \tag{3.10}$$

Note that as $\mathrm{tr}\{\rho_{th}\} = 1$, it follows that $Z = \mathrm{tr}\left\{e^{-\beta H}\right\}$. Therefore,

$$\rho_{th} = \frac{e^{-\beta H}}{\mathrm{tr}\{e^{-\beta H}\}}. \tag{3.11}$$

To find β let us calculate the entropy

$$\begin{aligned} S &= -k_B \operatorname{tr}\{\rho_{th} \ln \rho_t h\} \\ &= -k_B \left(\sum_i p_i \ln e^{-\beta E_i} - \sum_i p_i \ln Z \right) \\ &= k_B \beta \sum_i p_i E_i - k_B \ln Z \sum_i p_i \\ &= k_B \beta U - k_B \ln Z, \end{aligned} \tag{3.12}$$

differentiating S in relation to the average energy U, knowing that $\frac{\partial S}{\partial U} = \frac{1}{T}$, we have

$$\frac{\partial S}{\partial U} = k_B \beta = \frac{1}{T} \rightarrow \beta = \frac{1}{k_B T} \tag{3.13}$$

the Equation 3.11 represent the state of maximum entropy, where the probabilities don't change with time and $\beta = 1/k_B T$.

The master equation is used to describe the interaction between the system and the reservoir, being a tool that describes the evolution of open quantum systems. This equation is a generalization of the Schrödinger Equation, which normally describes the evolution of isolated systems [18]. The total Hamiltonian is given by:

$$H = H_S + H_R + H_{SR}, \tag{3.14}$$

where H_S, H_R e H_{RS} are respectively the Hamiltonian of the system, the reservoir, and the interaction between both. Changing to the interaction picture, the von Neumann Equation is

$$\dot{\tilde{\rho}}(t) = -\frac{i}{\hbar} \left[\tilde{H}_I(t), \tilde{\rho}(t) \right], \tag{3.15}$$

by integrating $\tilde{\rho}(t)$, we obtain

$$\tilde{\rho}(t) = \tilde{\rho}(0) - i \int_0^t dt' \left[\tilde{H}_I(t'), \tilde{\rho}(t') \right]. \tag{3.16}$$

Taking the partial trace allows one to obtain the system's state, denoted as $\tilde{\rho}_S$

$$\frac{d}{dt}\tilde{\rho}_S(t) = -\frac{i}{\hbar^2} \int_0^t dt' tr_R \left[\tilde{H}_I(t), \left[\tilde{H}_I(t'), \rho(t') \right] \right], \tag{3.17}$$

assuming that

$$\operatorname{tr}_R \left[H_I(t), \rho(0) \right] = 0, \tag{3.18}$$

which means that initially, as the system has not yet interacted with the reservoir, the trace is zero.

Here, we will make the first of a series of approximations to obtain the Markovian

Master Equation. In this approximation, known as the Born approximation, we assume that the coupling between the system and the reservoir is weak, such that the influence of the system on the reservoir is small [19]. Thus, the density matrix of the reservoir, ρ_R, is not affected by the interaction, and the state of the total system at time t can be approximately described by:

$$\rho(t) \approx \rho_S(t) \otimes \rho_R, \tag{3.19}$$

Therefore

$$\dot{\tilde{\rho}}_S(t) = -\frac{i}{\hbar^2} \int_0^t dt' \, \mathrm{tr}_R \left[\tilde{H}_I(t), \left[\tilde{H}_I(t'), \rho_S(t') \otimes \rho_R \right] \right]. \tag{3.20}$$

To simplify the expression, we will make a second approximation, known as the Markov approximation, which involves considering that the state of the system does not depend on the past. This means $\rho_S(t') \approx \rho_S(t)$, and thus,

$$\dot{\tilde{\rho}}_S(t) = -\frac{i}{\hbar^2} \int_0^t dt' \, \mathrm{tr}_R \left[\tilde{H}_I(t), \left[\tilde{H}_I(t'), \rho_S(t) \otimes \rho_R \right] \right]. \tag{3.21}$$

Consider a Hamiltonian representing the interaction between the reservoir and the system:

$$H_I = \sum_\alpha s_\alpha \otimes R_\alpha \tag{3.22}$$

where s_α are operators in the Hilbert space of S, and the R_α are reservoir operators in the Hilbert space of R. In the interaction picture, we have:

$$\tilde{H}_I(t) = \sum_\alpha \tilde{s}_\alpha(t) \tilde{R}_\alpha(t). \tag{3.23}$$

Expanding the commutator and substituting Equation 3.23 into 3.21, we obtain:

$$\begin{aligned} \dot{\tilde{\rho}}_S(t) = -\sum_{\alpha,\beta} \int_0^t dt' \Big\{ & \tilde{s}_\alpha(t)\tilde{s}_\beta\,(t')\tilde{\rho}_S(t)\,\mathrm{tr}_R[\tilde{R}_\alpha(t)\tilde{R}_\beta(t')\tilde{\rho}_B] \\ & - \tilde{s}_\alpha(t)\tilde{\rho}_S(t)\tilde{s}_\beta(t')\,\mathrm{tr}_R[\tilde{R}_\alpha(t)\tilde{\rho}_B\tilde{R}_\beta(t')] \\ & - \tilde{s}_\beta(t')\tilde{\rho}_S(t)\tilde{s}_\alpha(t)\,\mathrm{tr}_R[\tilde{R}_\beta(t')\tilde{\rho}_B\tilde{R}_\alpha(t)] \\ & + \tilde{\rho}_S(t)\tilde{s}_\beta(t')\tilde{s}_\alpha(t)\,\mathrm{tr}_R[\tilde{\rho}_B\tilde{R}_\beta(t')\tilde{R}_\alpha(t)] \Big\}, \end{aligned} \tag{3.24}$$

Using the cyclical property of the trace, we can rewrite it as:

$$\begin{aligned} \dot{\tilde{\rho}}_S(t) = -\sum_{\alpha,\beta} \int_0^t dt' \Big\{ & [\tilde{s}_\alpha(t)\tilde{s}_\beta\,(t')\tilde{\rho}_S(t) - \tilde{s}_\beta(t')\tilde{\rho}_S(t)\tilde{s}_\alpha(t)] \left\langle \tilde{R}_\alpha(t)\tilde{R}_\beta(t') \right\rangle_R \\ & + [\tilde{\rho}_S(t)\tilde{s}_\beta(t')\tilde{s}_\alpha(t) - \tilde{s}_\alpha(t)\tilde{\rho}_S(t)\tilde{s}_\beta(t')] \left\langle \tilde{R}_\beta(t')\tilde{R}_\alpha(t) \right\rangle_r \Big\}, \end{aligned} \tag{3.25}$$

where the correlation functions are given by:

$$\left\langle \tilde{R}_\alpha(t)\tilde{R}_\beta(t')\right\rangle_R = \mathrm{tr}_R[\tilde{\rho}_R\tilde{R}_\alpha(t)\tilde{R}_\beta(t')], \tag{3.26}$$

and

$$\left\langle \tilde{R}_\beta(t')\tilde{R}_\alpha(t)\right\rangle_R = \mathrm{tr}_R[\tilde{\rho}_R\tilde{R}_\beta(t')\tilde{R}_\alpha(t)]. \tag{3.27}$$

Considering now a system of a two level atom damped by a reservoir of oscillators the Hamiltonian that describe this situation using the rotate wave approximation is

$$H = \frac{1}{2}\hbar\omega_0\sigma_z + \sum_j \omega_j a_j^\dagger a_j + \hbar\sum_j(\kappa_j^*\sigma_- a_j^\dagger + \kappa_j\sigma_+ a_j). \tag{3.28}$$

The first term in the Hamiltonian describes the system, specifically a two-level atom, while the second term represents a reservoir of harmonic oscillators. The term $\kappa_j^*\sigma_- a_j^\dagger$ describes the process where the atom transitions from the higher energy state to the lower energy state, simultaneously generating a photon in mode j. Conversely, $\kappa\sigma_+ a_j$ describes the reverse process, where the atom shifts from the lower energy state to the higher energy state, emitting a photon in mode j. Here, κ_j represents the coupling constant between the system and the reservoir. The σ_- operator is responsible for driving the atom from the higher state to the lower state, while the σ_+ operator accomplishes the reverse, transitioning the atom from the lower state to the higher state.

In this context, we consider the operators s_α as $s_1 = \sigma_-$ and $s_2 = \sigma_+$, and the operators R_α as $R_1 = \sum_j \kappa_j^* a_j^\dagger$ and $R_2 = \sum_j \kappa_j a_j$. For the interaction picture we using the following transformations:

$$\tilde{s}_1 = \sigma_- e^{-i\omega_0 t} \tag{3.29}$$

$$\tilde{s}_2 = \sigma_+ e^{i\omega_0 t} \tag{3.30}$$

$$\tilde{R}_1 = \sum_j \kappa_j^* a_j^\dagger e^{i\omega_j t} \tag{3.31}$$

$$\tilde{R}_2 = \sum_j \kappa_j a_j e^{-i\omega_j t} \tag{3.32}$$

by substituting these definitions into Equation 3.25, we can rewrite the equation as:

$$\begin{aligned}\dot{\tilde{\rho}}_S(t) = -\int_0^t dt' \Big\{ &[\sigma_-\sigma_-\tilde{\rho}_S(t) - \sigma_-\tilde{\rho}_S(t)\sigma_-]e^{-i\omega_0(t+t')}\left\langle \tilde{R}_1(t)\tilde{R}_1(t')\right\rangle_R + \text{h.c} \\ &- [\tilde{\rho}_S(t)\sigma_-\sigma_- - \sigma_-\tilde{\rho}_S(t)\sigma_-]e^{-i\omega_0(t+t')}\left\langle \tilde{R}_1(t')\tilde{R}_1(t)\right\rangle_R + \text{h.c} \\ &- [\sigma_-\sigma_+\tilde{\rho}_S(t) - \sigma_+\tilde{\rho}_S(t)\sigma_-]e^{-i\omega_0(t-t')}\left\langle \tilde{R}_1(t)\tilde{R}_2(t')\right\rangle_R + \text{h.c} \\ &- [\tilde{\rho}_S(t)\sigma_+\sigma_- - \sigma_-\tilde{\rho}_S(t)\sigma_+]e^{-i\omega_0(t-t')}\left\langle \tilde{R}_2(t')\tilde{R}_1(t)\right\rangle_R + \text{h.c}\Big\},\end{aligned} \tag{3.33}$$

where "h.c." denotes the Hermitian conjugate. The reservoir correlation functions are expressed in terms of the trace using the Fock states as a basis, which is an orthogonal

basis:

$$\left\langle \tilde{R}_1(t)\tilde{R}_1(t')\right\rangle_R = \sum_{j,k} \kappa_j^* \kappa_k^* e^{i(\omega_j t+\omega_k t')} \operatorname{tr}\left[\rho_R a_j^\dagger a_k^\dagger\right] = 0, \tag{3.34}$$

$$\left\langle \tilde{R}_2(t)\tilde{R}_2(t')\right\rangle_R = \sum_{j,k} \kappa_j \kappa_k e^{-i(\omega_j t+\omega_k t')} \operatorname{tr}[\rho_R a_j a_k] = 0, \tag{3.35}$$

$$\left\langle \tilde{R}_1(t)\tilde{R}_2(t')\right\rangle_R = \sum_{j,k} \kappa_j^* \kappa_k e^{i(\omega_j t-\omega_k t')} \operatorname{tr}\left[\rho_R a_j^\dagger a_k\right] = \sum_j |\kappa_j|^2 e^{i\omega_j(t-t')}\bar{n}(\omega_j,T), \tag{3.36}$$

$$\left\langle \tilde{R}_2(t)\tilde{R}_1(t')\right\rangle_R = \sum_{j,k} \kappa_j^* \kappa_k e^{i(\omega_j t-\omega_k t')} \operatorname{tr}\left[\rho_R a_j^\dagger a_k\right] = \sum_j |\kappa_j|^2 e^{i\omega_j(t-t')}[\bar{n}(\omega_j,T)-1], \tag{3.37}$$

in which $\bar{n}(\omega_j, T)$ corresponds to the number of photons for an oscillator with frequency ω_j in thermal equilibrium at temperature T

$$\bar{n}(\omega_j,T) = \operatorname{tr}\left[\rho_B a_j^\dagger a_j\right] = \frac{1}{e^{\hbar\omega_j/k_BT}-1}. \tag{3.38}$$

Now, by making a change of variable $\tau = t - t'$

$$\begin{aligned}\frac{d\tilde{\rho}(t)}{dt} = -\int_0^t d\tau \Big\{ &[\sigma_-\sigma_+\tilde{\rho}(t) - \sigma_+\tilde{\rho}(t)\sigma_-]\, e^{-i\omega_0\tau}\left\langle \tilde{R}^\dagger(t)\tilde{R}(t-\tau)\right\rangle_R \\ &+ [\tilde{\rho}(t)\sigma_+\sigma_- - \sigma_-\tilde{\rho}(t)\sigma_+]\, e^{-i\omega_0\tau}\left\langle \tilde{R}(t-\tau)\tilde{R}^\dagger(t)\right\rangle_R \\ &+ [\sigma_+\sigma_-\tilde{\rho}(t) - \sigma_-\tilde{\rho}(t+\tau)\sigma_+]\, e^{i\omega_0\tau}\left\langle \tilde{R}(t)\tilde{R}^\dagger(t-\tau)\right\rangle_R \\ &+ [\tilde{\rho}(t)\sigma_-\sigma_+ - \sigma_+\tilde{\rho}(t)\sigma_-]\, e^{i\omega_0\tau}\left\langle \tilde{R}^\dagger(t-\tau)\tilde{R}(t)\right\rangle_R \Big\},\end{aligned} \tag{3.39}$$

note that the change of variable does not affect $\tilde{\rho}(t)$ due to the Markovian approximation we had made. Replacing the sum with an integral, we introduce a density of states function, now the correlation functions are:

$$\begin{aligned}\left\langle \tilde{R}^\dagger(t)\tilde{R}(t-\tau)\right\rangle_R &= \int_0^\infty d\omega g(\omega)|\kappa(\omega)|^2 e^{i\omega\tau}\bar{n}(\omega,\beta), \\ \left\langle \tilde{R}(t-\tau)\tilde{R}^\dagger(t)\right\rangle_R &= \int_0^\infty d\omega g(\omega)|\kappa(\omega)|^2 e^{i\omega\tau}[1-\bar{n}(\omega,\beta)], \\ \left\langle \tilde{R}(t)\tilde{R}^\dagger(t-\tau)\right\rangle_R &= \int_0^\infty d\omega g(\omega)|\kappa(\omega)|^2 e^{-i\omega\tau}[1-\bar{n}(\omega,\beta)], \\ \left\langle \tilde{R}^\dagger(t-\tau)\tilde{R}(t)\right\rangle_R &= \int_0^\infty d\omega g(\omega)|\kappa(\omega)|^2 e^{-i\omega\tau}\bar{n}(\omega,\beta).\end{aligned} \tag{3.40}$$

Making the following definitions:

$$\begin{aligned}A &\equiv \int_0^t d\tau \int_0^\infty d\omega g(\omega)|\kappa(\omega)|^2 e^{i(\omega-\omega_0)\tau}, \\ B &\equiv \int_0^t d\tau \int_0^\infty d\omega g(\omega)|\kappa(\omega)|^2 e^{i(\omega-\omega_0)\tau}\bar{n}(\omega,\beta),\end{aligned} \tag{3.41}$$

so, we can rewrite

$$\begin{aligned}\dot{\tilde{\rho}}(t) = &A\left[\sigma_-\tilde{\rho}(t)\sigma_+ - \sigma_+\sigma_-\tilde{\rho}(t)\right] + B\left[\sigma_-\tilde{\rho}(t)\sigma_+ + \sigma_+\tilde{\rho}(t)\sigma_- - \sigma_+\sigma_-\tilde{\rho}(t) - \tilde{\rho}(t)\sigma_-\sigma_+\right] \\ &+ A^*\left[\sigma_+\tilde{\rho}(t)\sigma_- - \sigma_-\sigma_+\tilde{\rho}(t)\right] + B^*\left[\sigma_+\tilde{\rho}(t)\sigma_- + \sigma_-\tilde{\rho}(t)\sigma_+ - \sigma_-\sigma_+\tilde{\rho}(t) - \tilde{\rho}(t)\sigma_+\sigma_-\right].\end{aligned} \tag{3.42}$$

Given that the reservoir's dynamics occur significantly faster than those of the system, we can extend the integration limit to infinity,

$$\lim_{t\to\infty}\int_0^t d\tau e^{i(\omega-\omega_0)\tau} = \pi\delta\left(\omega-\omega_0\right) + i\frac{P}{\omega_0-\omega}, \tag{3.43}$$

where P denotes the Cauchy principal value. Thus, by using the property of filtering of the delta distribution, we have:

$$\begin{aligned}A &= \pi g\left(\omega_0\right)\left|\kappa\left(\omega_0\right)\right|^2 + i\Delta, \\ B &= \pi g\left(\omega_0\right)\left|\kappa\left(\omega_0\right)\right|^2\bar{n}(\omega,\beta) + i\Delta',\end{aligned} \tag{3.44}$$

where Δ and Δ' are given by:

$$\begin{aligned}\Delta &= P\int_0^\infty d\omega\frac{g(\omega)|\kappa(\omega)|^2}{\omega_0-\omega}, \\ \Delta' &= P\int_0^\infty d\omega\frac{g(\omega)|\kappa(\omega)|^2}{\omega_0-\omega}\bar{n}(\omega,\beta).\end{aligned} \tag{3.45}$$

If we define $\gamma = 2\pi g\left(\omega_0\right)\left|\kappa\left(\omega_0\right)\right|^2$ and $\bar{n} = \bar{n}(\omega,\beta)$, then:

$$\begin{aligned}\dot{\tilde{\rho}}(t) = -i(2\Delta'+\Delta)\left[\sigma_z,\tilde{\rho}(t)\right] + &\frac{\gamma}{2}(\bar{n}+1)\left(2\sigma_-\tilde{\rho}(t)\sigma_+ - \sigma_+\sigma_-\tilde{\rho}(t) - \tilde{\rho}(t)\sigma_+\sigma_-\right) \\ &+ \frac{\gamma}{2}\bar{n}\left(2\sigma_+\tilde{\rho}(t)\sigma_- - \sigma_-\sigma_+\tilde{\rho}(t) - \tilde{\rho}(t)\sigma_-\sigma_+\right).\end{aligned} \tag{3.46}$$

Returning to the Schrödinger representation using:

$$\dot{\rho} = \frac{1}{i\hbar}[H_S,\rho] + e^{-(i/\hbar)H_S t}\dot{\tilde{\rho}}(t)e^{(i/\hbar)H_S t}, \tag{3.47}$$

we can rewrite it as:

$$\begin{aligned}\dot{\rho}(t) = &-i\omega'_A\left[\sigma_z,\rho(t)\right] + \frac{\gamma}{2}(\bar{n}+1)\left(2\sigma_-\rho(t)\sigma_+ - \sigma_+\sigma_-\rho(t) - \rho(t)\sigma_+\sigma_-\right) \\ &+ \frac{\gamma}{2}\bar{n}\left(2\sigma_+\rho(t)\sigma_- - \sigma_-\sigma_+\rho(t) - \rho(t)\sigma_-\sigma_+\right).\end{aligned} \tag{3.48}$$

where

$$\omega'_A \equiv \omega_A + 2\Delta' + \Delta.$$

Note that there is a frequency shift of the atom due to its dependence on the reservoir's

temperature, which appears in $2\Delta'$. Commonly when we study open quantum systems through master equations, it is often assumed that the Lamb shift Hamiltonian is insignificant [20], with this we have:

$$\dot{\rho}(t) = \frac{1}{i\hbar}\left[H_S, \rho(t)\right] + \frac{\gamma}{2}(\bar{n}+1)\mathcal{D}[\sigma_-]\rho(t) + \frac{\gamma}{2}\bar{n}\mathcal{D}[\sigma_+]\rho(t) \tag{3.49}$$

where $\mathcal{D}[X]\rho \equiv 2X\rho(t)X^\dagger - X^\dagger X\rho(t) - \rho(t)X^\dagger X$. Or simply as

$$\frac{d\rho(t)}{dt} = \frac{1}{i\hbar}\left[H_S, \rho(t)\right] + \mathcal{D}(\rho), \tag{3.50}$$

where $\mathcal{D}(\rho)$ is known as the dissipator. Equation 3.50 reveals that the dynamics of the system is governed by a term that depends exclusively on the system's Hamiltonian, while the other term indicates that the changes that affect the dynamics depend only on the characteristics of the reservoir.

The asymptotic state of Equation 3.49, which is the solution when $\dot{\rho}(t \to \infty) = 0$, represents a state of thermal equilibrium between a reservoir at temperature T and a two-level atom system, expressed as

$$\rho(t \to \infty) = \frac{e^{-\beta\hbar\omega_A\sigma_z/2}}{2\cosh\beta\hbar\omega_A/2}. \tag{3.51}$$

Fermionic reservoirs refer to a set of non-interacting fermionic particles, which obey the Fermi-Dirac statistics. This type of reservoir is of interest because it admits a negative effective temperature. This occurs because the temperature can be defined according to the statistical distribution of the particles, in conditions where the inversion of the energy population can result in a negative effective temperature [17].

Let the Hamiltonian describing the reservoir be:

$$H_R = \frac{\hbar}{2}\sum_j \omega_j \sigma_{z,j} \tag{3.52}$$

In the scenario where a system is weakly coupled to a fermionic reservoir the system dynamics is given by:

$$\begin{aligned}\dot{\rho}(t) = &- i\omega'_A\left[\sigma_z, \rho(t)\right] + \frac{\gamma}{2}(1-\bar{n_f})\left(2\sigma_-\rho(t)\sigma_+ - \sigma_+\sigma_-\rho(t) - \rho(t)\sigma_+\sigma_-\right) \\ &+ \frac{\gamma}{2}\bar{n_f}\left(2\sigma_+\rho(t)\sigma_- - \sigma_-\sigma_+\rho(t) - \rho(t)\sigma_-\sigma_+\right),\end{aligned} \tag{3.53}$$

where $\bar{n_f}$ is the average number of electrons in the excited state of atom, which obeys the Fermi-Dirac distribution [21]. In the Appendix A we present details to obtain the Equation 3.53.

3.2 Laws of Quantum Thermodynamics

To introduce the first law of thermodynamics for isolated quantum systems or those weakly coupled to a reservoir, it is important to establish the definitions for work and heat. In this regard, we will adhere to the definition put forth by R. Alicki [22]. To proceed with this, let us consider entropy as given by:

$$S(t) = k_B S_{vN} = k_B \,\mathrm{tr}\{\rho(t)\ln\rho(t)\}, \tag{3.54}$$

In the case of an equilibrium state, it corresponds to the Gibbs entropy [23]. The energy of the system is:

$$E(t) = \mathrm{tr}\{H(t)\rho(t)\}, \tag{3.55}$$

differentiating Equation 3.55 with respect to time yields

$$\frac{dE(t)}{dt} = \mathrm{tr}\left\{\frac{dH(t)}{dt}\rho(t)\right\} + \mathrm{tr}\left\{H(t)\frac{d\rho(t)}{dt}\right\}. \tag{3.56}$$

According to [22], we will identify work and heat as

$$W = \int_0^\tau \mathrm{tr}\left\{\frac{dH(t)}{dt}\rho(t)\right\}dt, \tag{3.57}$$

and

$$Q = \int_0^\tau \mathrm{tr}\left\{H(t)\frac{d\rho(t)}{dt}\right\}dt, \tag{3.58}$$

Where τ is the time of evolution, and changes in the Hamiltonian correspond to alterations induced by external forces, this leads us to identify Equation 3.57 as work. With these definitions, we have the first law as

$$\Delta E = W + Q. \tag{3.59}$$

Now, considering that the change in entropy is given by

$$dS = dS' + d\Sigma, \tag{3.60}$$

where dS' is the entropy exchange between the system and the reservoir, and $d\Sigma$ is the entropy production of the system. Defining the entropy flow per unit time interval as

$$J = \beta\frac{dQ}{dt}, \tag{3.61}$$

substituting 3.58 into 3.61, and considering $d\rho(t)/dt$ as presented in 3.50, we have

$$\begin{aligned} J &= \beta \left(\frac{1}{i\hbar} \operatorname{tr}\{[H,\rho]H\} + \operatorname{tr}\{\mathcal{D}(\rho)\}H \right) \\ &= \beta \left(\frac{1}{i\hbar} \operatorname{tr}\{H\rho H - \rho H H\} + \operatorname{tr}\{\mathcal{D}(\rho)\}H \right), \end{aligned} \tag{3.62}$$

using the cyclic property of the trace, we obtain

$$J = \beta \operatorname{tr}\{\mathcal{D}(\rho)H\}. \tag{3.63}$$

The rate of entropy production, denoted as $\sigma(t)$, can be defined as the difference between the total entropy of the system and the entropy flow from the reservoir

$$\sigma(t) = \frac{dS}{dt} - J, \tag{3.64}$$

using Equation 3.60 and 3.63 in the Equation 3.64

$$\begin{aligned} \sigma(t) &= \frac{d}{dt}\left(-\operatorname{tr}\{\rho \ln \rho\}\right) - \beta \operatorname{tr}\{\mathcal{D}(\rho)H\} \\ &= -\operatorname{tr}\left\{ \frac{d\rho}{dt} \ln \rho \right\} + \operatorname{tr}\left\{ \rho\rho^{-1} \frac{d\rho}{dt} \right\} - \beta \operatorname{tr}\{\mathcal{D}(\rho)H\} \\ &= -\operatorname{tr}\left\{ \left(\frac{1}{i\hbar}[H,\rho] \right) \ln \rho \right\} - \operatorname{tr}\{\mathcal{D}(\rho)\ln\rho\} - \beta \operatorname{tr}\{\mathcal{D}(\rho)H\}, \end{aligned} \tag{3.65}$$

once again utilizing the cyclic property of the trace and the fact that $[\rho, \ln\rho] = 0$, the first term becomes zero, thus

$$\sigma(t) = -\operatorname{tr}\{\mathcal{D}(\rho)(\ln\rho + \beta H)\}. \tag{3.66}$$

The rate of entropy exchanged with the reservoir can be identified as

$$\frac{dS'}{dt} = \beta \frac{dQ}{dt} = \beta \operatorname{tr}\{\mathcal{D}(\rho)H\}, \tag{3.67}$$

once $S = -\operatorname{tr}\{\rho \ln \rho\}$, we have

$$\frac{dS}{dt} = -\operatorname{tr}\{\mathcal{D}(\rho)\ln\rho\}. \tag{3.68}$$

Therefore

$$\frac{d\Sigma}{dt} = \frac{dS}{dt} - \frac{dS'}{dt} = \sigma(t), \tag{3.69}$$

considering $\beta H = \ln \rho_{th} + \ln Z$, where ρ_{th} is the thermal state of ρ, we can substitute this into Equation 3.66

$$\sigma(t) = -\operatorname{tr}\{\mathcal{D}(\rho)(\ln\rho + \ln\rho_{th} + \ln Z)\}, \tag{3.70}$$

substituting also $\mathcal{D}(\rho) = \dot{\rho} - \frac{1}{i\hbar}[H,\rho]$

$$\begin{aligned}\sigma(t) &= -\operatorname{tr}\left\{\left(\frac{d\rho}{dt} - \frac{1}{i\hbar}[H,\rho]\right)\ln\rho\right\} + \operatorname{tr}\left\{\left(\frac{d\rho}{dt} - \frac{1}{i\hbar}[H,\rho]\right)\ln\rho_{th}\right\}, \\ &= -\operatorname{tr}\left\{\frac{d\rho}{dt}\ln\rho\right\} + \operatorname{tr}\left\{\frac{d\rho}{dt}\ln\rho_{th}\right\}.\end{aligned} \tag{3.71}$$

Note that

$$-\operatorname{tr}\left\{\frac{d}{dt}(\rho\ln\rho)\right\} = -\operatorname{tr}\left\{\frac{d\rho}{dt}\ln\rho\right\}, \tag{3.72}$$

then

$$-\operatorname{tr}\left\{\frac{d}{dt}(\rho\ln\rho)\right\} = -\operatorname{tr}\left\{\frac{d\rho}{dt}\ln\rho - \rho\rho^{-1}\frac{d\rho}{dt}\right\}, \tag{3.73}$$

so we can rewrite the Equation 3.71 as

$$\sigma(t) = -\operatorname{tr}\left\{\frac{d}{dt}\left(\rho\ln\rho - \rho\ln\rho_{th}\right)\right\} = -\frac{d}{dt}D(\rho||\rho_{th}). \tag{3.74}$$

Here, $D(\rho||\rho_{th}) = -(\rho\ln\rho - \rho\ln\rho_{th})$ represents the relative entropy, also known as entropy production, defined as Σ, and is always positive [6]. Thus, it is convenient to define the second law of thermodynamics for open quantum systems as:

$$\Sigma \geq 0. \tag{3.75}$$

The third law of thermodynamics is equally applicable in the quantum context, raising questions about the attainability of the ground state. When we consider an open quantum system, the third law prevents us from reaching a state of thermal equilibrium that corresponds to the system's ground state, as this would imply that this state would be at absolute zero temperature, violating the third law. These discussions are of great significance, as the ground state is often employed in the implementation of quantum algorithms, necessitating consideration of an initial error associated with the preparation of this state. The challenges in preparing the ground state are addressed in [2, 8, 9, 24].

3.3 The Third Law and The Cooling Rate

The Third Law of Thermodynamics, as previously mentioned, can be presented in two distinct approach. The first one is static a approach and is directly related to Nernst's heat theorem, postulating that, in the vicinity of absolute zero, all processes are isentropic, meaning the entropy change is constant. The second approach, based on the principle of the unattainability of absolute zero, adopts a dynamic perspective, stating that there is no cooling process in which it is possible to reach the minimum temperature in a finite time.

From a historical standpoint, the unattainability of absolute zero principle was introduced by Nernst as a necessary and sufficient condition for the validation of the heat theorem [15]. However, a study conducted by Masanes and Oppenheim [25] revealed a violation of this equivalence, emphasizing that this topic remains an open question.

Exploring the dynamic nature of the unattainability principle, Kosloff et al. [26] addressed the third law of thermodynamics in the context of quantum refrigerators. By studying these systems, they proposed an interpretation that links the cooling rate with unattainability. The result revealed that, under low-temperature conditions, the cooling rate converges to a power of order ζ, termed the characteristic factor:

$$\frac{dT_C}{dt} \sim -(Tc)^{\zeta}. \tag{3.76}$$

With $\zeta \geq 1$, the unattainability principle remains respected, as graphically demonstrated in Figure 3.1. The research conducted by Kosloff et al. plays a significant role in understanding the dynamic cooling processes in quantum systems. By analyzing the behavior of the temperature rate of change, we can assess the feasibility of reaching absolute zero.

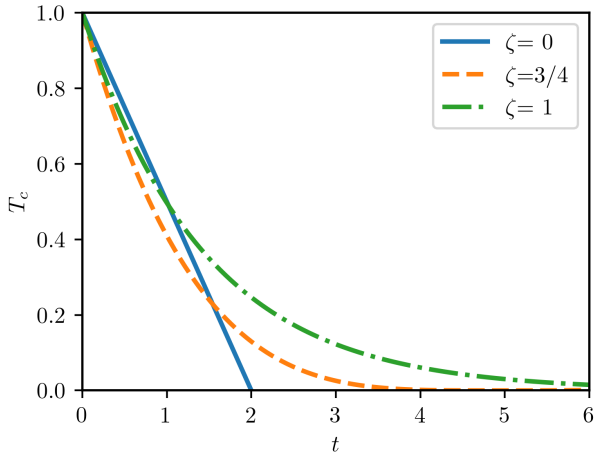

Figure 3.1: Temperature behavior in relation to cooling time for different values of ζ. Figure adapted from [2]

If we adopt $\zeta = 0$, the cooling rate remains constant, resulting in a linear relationship between T_C and time. Thus, there exists a finite time interval in which reaching absolute zero is possible. When $0 < \zeta < 1$, the behavior is no longer linear, but there is still a point in time where unattainability would be violated. Finally, for $\zeta = 1$, cooling the system to zero kelvin would require an infinite amount of time, aligning with the dynamic interpretation of the third law of thermodynamics.

It is important to emphasize that Kosloff developed this work in the context of quantum refrigerators, where T_C represents the cooling temperature associated with a

thermal equilibrium state. Additionally, the analysis of ζ is valid only for systems at low temperatures.

3.4 Quantum Otto Engine

In the quantum context, the Otto cycle functions similarly to the classical scenario. It involves two unitary stages, one for expansion and the other for compression, and two thermalization stages with the cold and hot reservoirs, respectively. Vamos abordar aqui o QOHE para um Two-Level System (TLS) cujas etapas são:

- Expansion: The expansion step takes place when a unitary transformation is applied, changing the frequency gap so that $\omega_c < \omega_h$, and also the Pauli matrix operators x and y. The state evolves with the unitary operator $U(\tau) = \mathcal{T}_+ e^{-(i/\hbar)\int_0^\tau H(t)dt}$, where $\mathcal{T}_+$ is the time-ordering operator. The system transitions from the initial equilibrium state ρ_c to the state ρ_{exp}.

$$\rho_c = \frac{e^{-\beta_c H_c}}{Z(\beta_c, \omega_c)} \xrightarrow{U(\tau)} \rho_{exp} = U(\tau)\rho_1 U^\dagger(\tau)$$

$$H_c = -\frac{\hbar\omega_c}{2}\sigma_x \rightarrow H_h = \frac{\hbar\omega_h}{2}\sigma_y.$$

  During this stage, there is no heat exchange with the reservoir, so all energy variation corresponds to the work performed during this step.

- Heating: The system is brought into contact with the hot reservoir, leaving the state ρ_{exp} to the thermal equilibrium state ρ_h, in this stage the Hamiltonian is kept constant and all energy variations correspond to the heat exchanged in the stage.

$$\rho_{exp} = U(\tau)\rho_c U^\dagger(\tau) \rightarrow \rho_h = \frac{e^{-\beta_h H_h}}{Z(\beta_h, \omega_h)}, \quad H_h = \frac{\hbar\omega_h}{2}\sigma_y.$$

- Compression: In a similar way to what occurs in the first stage, without allowing heat exchange, , which corresponds to the temporal reversal of the expansion stage described above.

$$\rho_h \frac{e^{-\beta_h H_h}}{Z(\beta_h, \omega_h)} \xrightarrow{V=U^\dagger(\tau)} \rho_{comp} = U^\dagger(\tau)\rho_h U(\tau)$$

$$H_h = \frac{\hbar\omega_h}{2}\sigma_y \rightarrow H_c = \frac{\hbar\omega_c}{2}\sigma_x.$$

- Cooling: After compression, the system is placed in contact with the cold reservoir, where heat exchange occurs, taking it from the ρ_{comp} state and returning to the

initial equilibrium state of the cycle, ρ_c

$$\rho_{comp} \to \rho_c = \frac{e^{-\beta_c H_c}}{Z(\beta_c, \omega_c)}, \quad H_c = \frac{\hbar\omega_c}{2}\sigma_x.$$

The cycle can be represented as in the following Figure 3.2

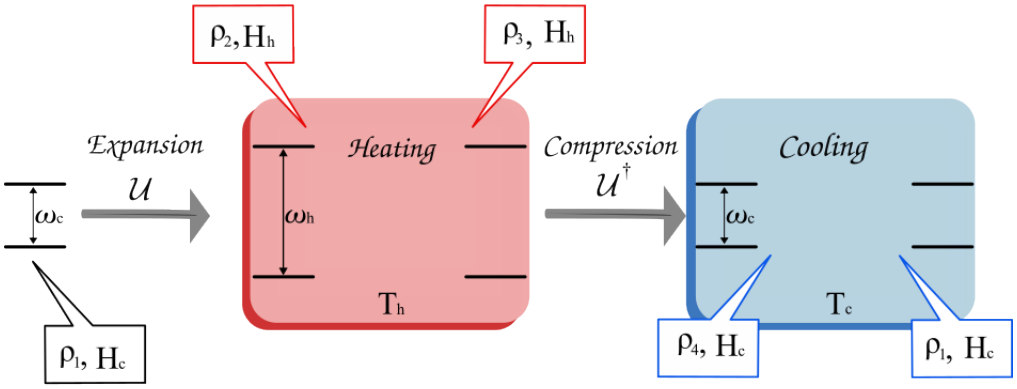

Figure 3.2: Representation of the Quantum Otto cycle.

For this cycle, heat and work are determined by the energy variation of each step [27].

$$W_{exp} = \mathrm{tr}\{H_h\rho_{exp}\} - \mathrm{tr}\{H_c\rho_c\}, \tag{3.77}$$

$$Q_h = \mathrm{tr}\{H_h(\rho_h - \rho_{exp})\}, \tag{3.78}$$

$$W_{comp} = \mathrm{tr}\{H_c\rho_c\} - \mathrm{tr}\{H_h\rho_{comp}\}, \tag{3.79}$$

$$Q_c = \mathrm{tr}\{H_c(\rho_c - \rho_{comp})\}. \tag{3.80}$$

Being $|e_x\rangle, |g_x\rangle$ the eigenstates of H_c, and $|e_y\rangle, |g_y\rangle$ the eigenstates of H_h, we can express the results of the above equations as [28]

$$W_{exp} = -\frac{\hbar}{2}(\omega_h - \omega_c)\tanh\frac{\hbar\beta_c\omega_c}{2} + \xi\hbar\omega\tanh\frac{\hbar\beta_c\omega_c}{2}, \tag{3.81}$$

$$W_{comp} = -\frac{\hbar}{2}(\omega_h - \omega_c)\tanh\frac{\hbar\beta_h\omega_h}{2} + \xi\hbar\omega\tanh\frac{\hbar\beta_h\omega_h}{2}, \tag{3.82}$$

$$Q_h = \frac{\hbar}{2}\omega_h\left[\tanh\frac{\hbar\beta_c\omega_c}{2} - \tanh\frac{\hbar\beta_h\omega_h}{2}\right] - \xi\hbar\omega_h\tanh\frac{\hbar\beta_c\omega_c}{2} \tag{3.83}$$

and

$$Q_c = -\frac{\hbar}{2}\omega_c\left[\tanh\frac{\hbar\beta_c\omega_c}{2} - \tanh\frac{\hbar\beta_h\omega_h}{2}\right] - \xi\hbar\omega_c\tanh\frac{\hbar\beta_h\omega_h}{2} \tag{3.84}$$

where $\xi \equiv |\langle g_y|U(\tau)|e_y\rangle|^2$ is the adiabaticity parameter, representing the probability of transitions between the eigenstates of $\langle g_y|$ and $|e_x\rangle$ or $\langle g_x|$ and $|e_y\rangle$. The adiabatic parameter can take values between zero, indicating, for example, that the state $\langle g_y|$ has

evolved to $\langle g_x|$ (this occurs when the evolution is carried out in the quasi-static regime), up to the value of 1/2, which occurs when the evolution is instantaneous, and the state remains unchanged. This parameter ξ provides information about the speed at which the expansion and compression stages occur, reflecting in the cycle period.

The net work of the cycle corresponds to the sum of the expansion and compression work

$$W = -\frac{\hbar(\omega_h - \omega_c)}{2}\left[\tanh\frac{\hbar\beta_c\omega_c}{2} - \tanh\frac{\hbar\beta_h\omega_h}{2}\right] + \xi\hbar\left[\tanh\frac{\hbar\beta_c\omega_c}{2} + \tanh\frac{\hbar\beta_h\omega_h}{2}\right]. \quad (3.85)$$

For the cycle to works as a motor, a necessary condition is $W < 0$ given the convention adopted so far. This implies that $\omega_h > \omega_c$ and $\xi \geq 0$. This condition also implies that

$$\frac{\omega_c}{\omega_h} > \frac{T_c}{T_h}. \quad (3.86)$$

As presented in Equation 2.13, we have that the efficiency is

$$\eta = 1 - \frac{\omega_c}{\omega_h}\left(\frac{1 + 2\xi\mathcal{F}}{1 - 2\xi\mathcal{G}}\right), \quad (3.87)$$

where

$$\mathcal{F} = \frac{\tanh\hbar\beta_h\omega_h/2}{\tanh\hbar\beta_c\omega_c/2 - \tanh\hbar\beta_h\omega_h/2} \quad (3.88)$$

and

$$\mathcal{G} = \frac{\tanh\hbar\beta_c\omega_c/2}{\tanh\hbar\beta_c\omega_c/2 - \tanh\hbar\beta_h\omega_h/2}. \quad (3.89)$$

Analyzing Equation 3.87, when $\xi = 0$, we have the efficiency of Otto as

$$\eta_{Otto} = 1 - \omega_c/\omega_h. \quad (3.90)$$

Considering that the engine operates in finite times $\xi > 0$, we can observe that the motor efficiency is reduced. Using the inequality in 3.86, we then have

$$\eta \leq \eta_{Otto} \leq \eta_c, \quad (3.91)$$

where $\eta_c = 1 - T_h/T_c$ is the efficiency of the Carnot heat engine. Note that even for quantum systems, the Carnot efficiency remains independent of the working substance, depending only on the temperatures of the reservoirs.

The studies on non-equilibrium thermodynamic processes began with the analysis of small perturbations in systems. From there, fluctuation theorems stood out, enabling the establishment of relationships between thermodynamic information even in systems far from equilibrium. Initially, these theorems were developed for classical systems [29] but were later extended to quantum systems [30], with experimental confirmation of

fluctuation relations in both types of systems [31].

The construction of fluctuation theorems involves two main ingredients. The first is related to the natural statistics of the system, requiring that the initial state of the system be in thermal equilibrium, described by a canonical distribution. The second requirement is linked to the system's dynamics, which must obey the principle of micro-reversibility, a characteristic of systems with temporal reversal symmetry [32].

3.5 Irreversibility in Quantum Systems

In this section, we will present an approach focused on quantum systems in the context of the fluctuation theorem. We will demonstrate how the Jarzynski equality emerges from the Tasaki-Crooks relation. Furthermore, we will explore the association of these relations with quantum friction and the ways in which they are related to the loss of useful energy during processes due to entropy production.

3.5.1 Tasaki-Crooks Relation

Let's consider a quantum process that we'll call the "forward" process, with a control parameter $\lambda(t)$ varying from $t = 0$ to $t = \tau$. These changes in the Hamiltonian go from $H(0)$ to $H(\tau)$. Also, consider another process, the "backward" process, in which the control parameter is $\tilde{\lambda}(\tau) = \lambda(\tau - t)$, corresponding to the change in the Hamiltonian from $H(\tau)$ to $H(0)$. Assuming that the system at the beginning of the "forward" process starts from a thermal equilibrium state $\rho_i^{eq} = e^{-\beta H(0)}/Z_i$ and in the "backward" process, it starts from the equilibrium state $\tilde{\rho}_\tau^{eq} = e^{-\beta H(\tau)}/Z\tau$, as depicted in the Figure 3.3

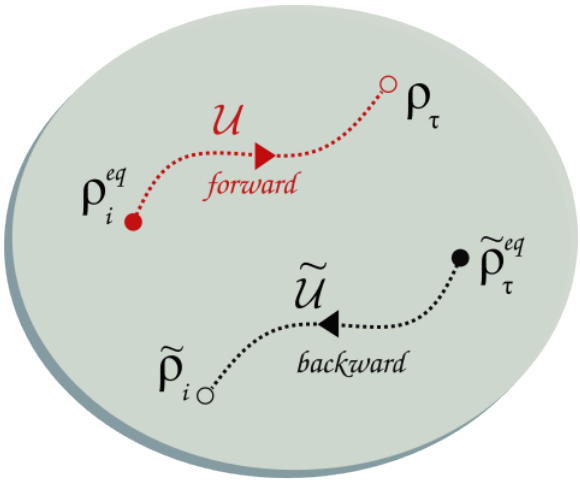

Figure 3.3: Forward and Backward process.

Starting from the definition of probability distribution of work [32]

$$P(W) := \sum_{m,n} p_n^i p_{m|n}^\tau \delta(W - \Delta_{m,n}), \tag{3.92}$$

where p_n^i is the probability of finding the system in the state $|n\rangle$ with energy E_n at the initial time, $p_{m|n}^\tau = |\langle m|\mathcal{U}_{0,\tau}|n\rangle|^2$ is the conditional probability that a transition from state $|n\rangle$ to state $|m\rangle$ has occurred during the application of the protocol, with $\mathcal{U}_{0,\tau}$ being the evolution operator. Finally, $\Delta_{m,n} = E_m - E_n$ is the energy difference between the initial and final eigenstates. The probability distribution of work for both the forward and backward processes

$$P_F(+W) = \sum_{m,n} p_n^i p_{m|n}^\tau \delta(W - E_m + E_n), \tag{3.93}$$

$$P_B(-W) = \sum_{m,n} p_m^\tau p_{n|m}^\tau \delta(-W - E_n + E_m), \tag{3.94}$$

with $p_{n|m}^\tau$ being the probability of transition, p_m^τ is the probability of the state having energy E_m at the initial time of the backward protocol. As a consequence of microreversibility [32], we have $p_{m|n}^\tau = p_{n|m}^\tau$, so we can write

$$P_F(+W) = \sum_{m,n} p_n^i p_{n|m}^\tau \delta(W - E_m + E_n), \tag{3.95}$$

Note that we can express $p_n^i = e^{-\beta E_n}/Z_i$ and also $\delta(x) = \delta(-x)$ so that

$$P_F(+W) = \frac{1}{Z_i} \sum_{m,n} e^{-\beta E_n} p_{n|m}^\tau \delta(-W + E_m - E_n), \tag{3.96}$$

considering $e^{-\beta E_m} = Z_\tau p_m^\tau$, we have

$$P_F(+W) = \frac{Z_\tau}{Z_i} \sum_{m,n} e^{-\beta(E_n - E_m)} p_m^\tau p_{n|m}^\tau \delta(-W + E_m - E_n), \tag{3.97}$$

also

$$P_F(+W) = \frac{Z_\tau}{Z_i} e^{\beta W} P_B(-W), \tag{3.98}$$

knowing that the Helmholtz free energy is given by $F = -\ln Z/\beta$, then $Z_i = e^{-\beta F_i}$. Thus, we obtain the Tasaki-Crooks relation:

$$\frac{P_F(+W)}{P_B(-W)} = e^{\beta(W - \Delta F)}. \tag{3.99}$$

We can obtain the Jarzynski equality using the Crooks relation, since

$$\left\langle e^{-\beta W} \right\rangle = \int e^{-\beta W} P_F(W) dW, \tag{3.100}$$

using Equation 3.99 in Equation 3.100

$$\left\langle e^{-\beta W} \right\rangle = \int e^{-\beta \Delta F} P_B(-W) dW, \tag{3.101}$$

as ΔF is independent of W and $\int P_B(-W)dW = 1$ since the work distribution is normalized, therefore

$$\left\langle e^{-\beta W} \right\rangle = e^{-\beta \Delta F} \tag{3.102}$$

Note that the Jarzynski equality allows us to obtain information about work, which is a quantity that depends on the process, knowing only the initial and final equilibrium states. Through the use of Jensen's inequality [33], this relation implies that

$$\langle W \rangle \geq \Delta F, \tag{3.103}$$

also intepreted as second law of themodinamics.

3.5.2 Irreversible Work

The irreversible work, denoted as $\langle W_{\text{irr}} \rangle$, can be represented as

$$\langle W_{irr} \rangle := \langle W \rangle - \Delta F \geq 0, \tag{3.104}$$

where $\langle W \rangle$ represents the work and ΔF is the change in the free energy due to a unitary transformation from $H(0)$ to $H(\tau)$. This irreversibility is quantified through the non-equilibrium entropy production, as introduced by [6]

$$\langle W_{irr} \rangle = \frac{1}{\beta} \Sigma, \tag{3.105}$$

where $\Sigma = D(\mathcal{U}_\tau \rho_i^{eq} \mathcal{U}_\tau^\dagger || \rho_\tau^{eq})$.

Let's analyze irreversible work in different scenarios. The first case considers a temporal dependence in the Hamiltonian, i.e., $[H(t), H(t')] \neq 0$, along with unitary transformations $\mathcal{U}(\tau)$ that can occur in both fast processes and processes following the quantum adiabatic theorem. The second case addresses irreversibility that arises even when $[H(t), H(t')] = 0$, becoming independent of the time τ at which the unitary transformation occurs.

In the first scenario, when the protocol occurs instantaneously, the temporal evolution operator tends to approach the identity operator, as discussed in [34]. In this case, the state remains practically unchanged, resulting in maximum entropy production. The faster the evolution, the higher the probability of transition, which we can term "Quantum Friction", as schematically depicted in Figure 3.4

Now, considering that the evolution follows the quantum adiabatic regime, i.e., when the process occurs in the quasi-static regime, entropy production is minimized. However, even when the transformation follows the adiabatic theorem, there is still entropy production. This is because, due to the change in the Hamiltonian, the final state after evolution does not correspond to a thermal equilibrium state with the Hamiltonian at the end of the expansion. This entropy production is known as *Residual Lag* or *Non-equilibrium Lag* [34].

The same occurs in the case where $[H(t), H(t')] = 0$, where the speed at which the transformation is carried out does not interfere with entropy production. Nevertheless, there is entropy production due to the fact that the system is out of equilibrium

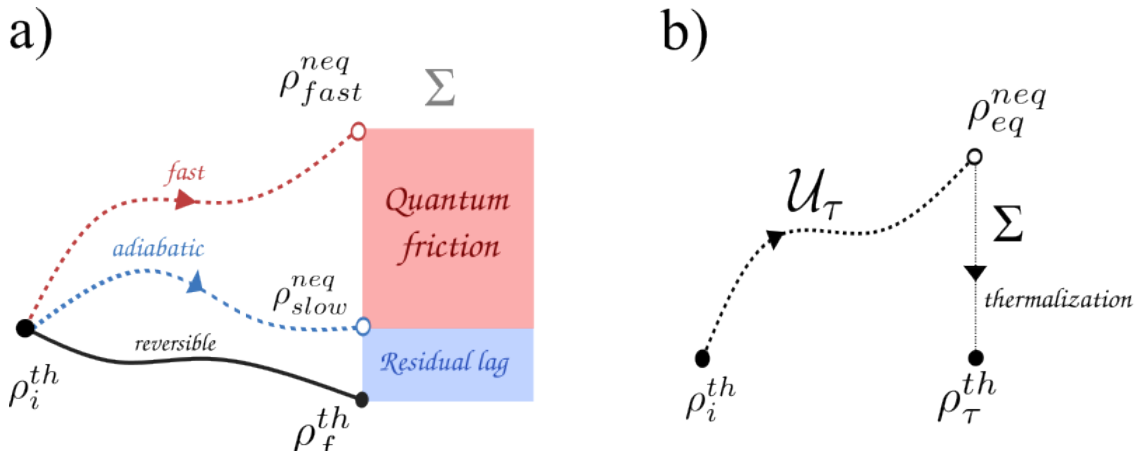

Figure 3.4: Production Entropy: a) The initial equilibrium state, ρ_i^{th}, can follow three paths: "fast," involving quantum friction; "adiabatic," leading to entropy production due to residual lag during thermalization; and "reversible," where no entropy production occurs. b) Schematic representation of entropy production, where the speed of the unitary transformation does not affect the amount of generated entropy.

The calculation of irreversible work in both scenarios is given via relative entropy. Irreversible work is also referred to as thermalization heat and can be interpreted as the exchange of energy between the system and the reservoir to reach a new thermal equilibrium state [6]. Considering the case where the system thermalizes with a reservoir at a temperature different from the temperature before the expansion, what Plastina et al, [6] calls Inner Friction, as schematically depicted in the following Figure

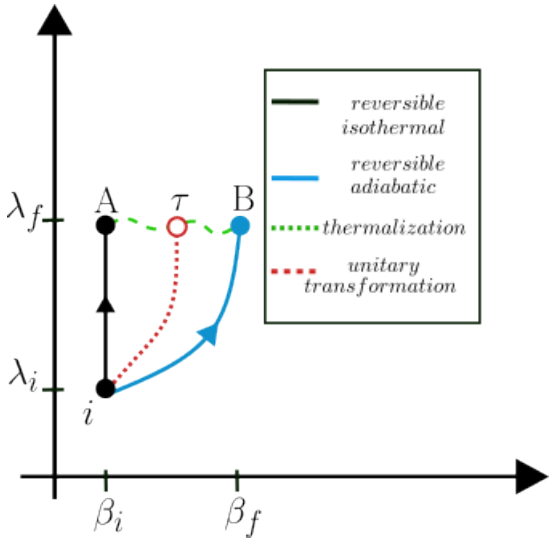

Figure 3.5: Schematic representation when there is a variation in a parameter λ. If this change occurs through a unitary transformation ($i \to \tau$) and then thermalization follows ($\tau \to B$), part of the energy change in this process is called friction work.

The system starts in a thermal state β_i, and at the end of the unitary transformation, the state becomes a non-equilibrium state ρ_τ. If the protocol were a reversible adiabatic process, the inner friction, characterized by

$$W_{fric} = \frac{1}{\beta_f} D(\rho_\tau || \rho_B), \tag{3.106}$$

this may be null because reversible adiabatic processes lack entropy production. It is worth mentioning that in the Otto cycle, the inner friction manifests itself both during the expansion and compression.

In the next chapter, we will perform the calculation of W_{fric} in the context of QOHE and investigate its influence on efficiency. Furthermore, we will examine the third law of thermodynamics in a process in which entropy is produced by "Residual Lag". All entropy production concepts presented so far will be applied exclusively to a two-level system.

CHAPTER 4

Results

The production of entropy, as we have seen, arises in different contexts, whether due to transitions during unitary evolutions or the intrinsic production of entropy associated with the thermalization entropy of the non-equilibrium state of the system. Applying this knowledge to the Quantum Otto Heat Engine (QOHE), we can observe that entropy production, typically responsible for the loss of useful work in heat engines, takes on a counterintuitive characteristic when dealing with a QOHE operating in a reservoir with effective negative temperature. We will demonstrate that this type of reservoir allows for conditions in which friction work, which would normally decrease useful work, contributes to the cycle's high performance. We will analyze our results based on the work developed by Assis et al. [35], thereby justifying the higher efficiency of the cycle presented in this same study.

Another result we will discuss here is the application of Nernst's theorem to a single qubit. We will introduce state functions analogous to enthalpy and Gibbs free energy, analyzing how these energies behave as the temperature approaches absolute zero. We will also address the behavior of thermal capacity and entropy production in this regime, aiming to extend, on a fundamental scale, Nernst's postulate, which forms the basis for the third law of thermodynamics. The results presented are derived from computational simulations and experimental data collected using NMR techniques.

4.1 Friction Work in QOHE

As observed earlier, we can calculate the friction work during the expansion stroke by examining the relative entropy between the state from quasi-static process ρ_{exp}^{qe} and the state of expansion ρ_{exp}

$$\left\langle W_{fric}^{exp} \right\rangle = \frac{1}{\beta_h^{qe}} D(\rho_{exp}||\rho_{exp}^{qe}). \tag{4.1}$$

Where the equilibrium state is

$$\rho_{exp}^{qe} = \frac{e^{\beta_h^{qe} h\nu_h \sigma_x/2}}{Z(\alpha_h^{qe})}, \tag{4.2}$$

with $\alpha_i = h\beta_i\nu_i/2$ and $i = c, h$, given that $\rho_{exp} = U\rho_c U^\dagger$, we consequently obtain:

$$\begin{aligned}
\left\langle W_{fric}^{exp} \right\rangle &= \frac{1}{\beta_h^{qe}} D(\rho_{exp}||\rho_{exp}^{qe}) \\
&= \frac{1}{\beta_h^{qe} Z_c} \operatorname{Tr}\left\{ U e^{\beta_c h\nu_c \sigma_y/2} U^\dagger \left[\ln\left(U \frac{e^{\beta_c h\nu_c \sigma_y/2}}{Z_c} U^\dagger \right) - \ln\left(\frac{e^{\beta_h^{qe} h\nu_h \sigma_x/2}}{Z_h^{qe}} \right) \right] \right\} \\
&= \frac{1}{\beta_h^{qe} Z_c} \operatorname{Tr}\left\{ U e^{\alpha_c \sigma_y} U^\dagger \left[U \ln\left(e^{\alpha_c \sigma_y} \right) U^\dagger - \ln\left(e^{\alpha_h^{qe} \sigma_x} \right) \right] \right\} + \ln\left(\frac{Z_h^{qe}}{Z_c} \right) \\
&= -\frac{\beta_c}{\beta_h^{qe}} \operatorname{Tr}\left(\rho_c H_c \right) + \frac{\beta_h \alpha_h^{qe}}{\beta_h^{qe} \alpha_h} \operatorname{Tr}\left(\rho_{exp} H_h \right) + \frac{1}{\beta_h^{qe}} \ln\left(\frac{Z_h^{qe}}{Z_c} \right) \\
&= \frac{\alpha_c}{\beta_h^{qe}} \tanh\left(\alpha_c \right) - \frac{\alpha_h^{qe}}{\beta_h^{qe}} \tanh\left(\alpha_c \right) (1 - 2\xi) + \frac{1}{\beta_h^{qe}} \ln\left(\frac{Z_h^{qe}}{Z_c} \right),
\end{aligned} \tag{4.3}$$

Calculating now for the compression stroke and considering the equilibrium state $\rho_{comp}^{qe} = \frac{e^{\beta_c^{qe} h\nu_c \sigma_y/2}}{Z(\alpha_c^{qe})}$, we have

$$\begin{aligned}
\left\langle W_{fric}^{comp} \right\rangle &= \frac{1}{\beta_c^{qe}} D(\rho_{comp}||\rho_{comp}^{qe}) \\
&= \frac{1}{\beta_c^{qe} Z_h} \operatorname{Tr}\left\{ V e^{\beta_h h\nu_h \sigma_x/2} V^\dagger \left[\ln\left(V \frac{e^{\beta_h h\nu_h \sigma_x/2}}{Z_h} V^\dagger \right) - \ln\left(\frac{e^{\beta_c^{qe} h\nu_c \sigma_y/2}}{Z_c^{qe}} \right) \right] \right\} \\
&= \frac{1}{\beta_c^{qe} Z_c} \operatorname{Tr}\left\{ V e^{\alpha_h \sigma_x} V^\dagger \left[V \ln\left(e^{\alpha_h \sigma_x} \right) V^\dagger - \ln\left(e^{\alpha_c^{qe} \sigma_x} \right) \right] \right\} + \ln\left(\frac{Z_c^{qe}}{Z_h} \right) \\
&= -\frac{\beta_h}{\beta_c^{qe}} \operatorname{Tr}\left(\rho_h H_h \right) + \frac{\beta_c \alpha_c^{qe}}{\beta_c^{qe} \alpha_c} \operatorname{Tr}\left(\rho_{comp} H_c \right) + \frac{1}{\beta_c^{qe}} \ln\left(\frac{Z_c^{qe}}{Z_h} \right) \\
&= \frac{\alpha_h}{\beta_c^{qe}} \tanh\left(\alpha_h \right) - \frac{\alpha_c^{qe}}{\beta_c^{qe}} \tanh\left(\alpha_h \right) (1 - 2\xi) + \frac{1}{\beta_c^{qe}} \ln\left(\frac{Z_c^{qe}}{Z_h} \right).
\end{aligned} \tag{4.4}$$

To perform these calculations, we utilized the cyclic property of the trace and the fact that $UU^\dagger = VV^\dagger = \mathbb{I}$. Note that, for the adiabatic expansion, the probabilities for the ground and excited states remain the same, that is,

$$\left.\begin{aligned} \langle g_y | \rho_c | g_y \rangle &= \left\langle g_x \left| \rho_{exp}^{qe} \right| g_x \right\rangle \\ \langle e_y | \rho_c | e_y \rangle &= \left\langle e_x \left| \rho_{exp}^{qe} \right| e_x \right\rangle \end{aligned}\right\} \Longrightarrow \alpha_h^{qe} = \alpha_c,$$

Similarly, for the compression, we obtain $\alpha_c^{qe} = \alpha_h$. Using this relation, we can find the total work over the cycle using $\langle W_{fric} \rangle = \left\langle W_{fric}^{exp} \right\rangle + \left\langle W_{fric}^{comp} \right\rangle$, meaning

$$\langle W_{fric} \rangle = h\xi \left(\nu_c \tanh \frac{\beta_h h\nu_h}{2} + \nu_h \tanh \frac{\beta_h h\nu_h}{2} \right). \tag{4.5}$$

When comparing Equation (4.5) with Equation (3.85), it is possible to note that the total

friction work corresponds exactly to the second term in the total work sum, with the first term being the quasi-static work.

$$\langle W\rangle = \langle W^{\text{ad}}\rangle + \langle W^{\text{fric}}\rangle = -\frac{h}{2}(\nu_h - \nu_c)\left[\tanh\left(\frac{1}{2}\beta_c h\nu_c\right) + \tanh\left(\frac{1}{2}\beta_h h\nu_h\right)\right] + h\xi\left[\nu_c \tanh\left(\frac{1}{2}\beta_h h\nu_h\right) + \nu_h \tanh\left(\frac{1}{2}\beta_c h\nu_c\right)\right] \tag{4.6}$$

The equation above can still be written in terms of populations:

$$\tanh\left(\alpha_{h/c}\right) = \tanh\left(\frac{1}{2}\ln\frac{1-p^e_{h/c}}{p^e_{h/c}}\right) = \frac{\left(\frac{1-p^e_{h/c}}{p^e_{h/c}}\right)^{1/2} - \left(\frac{p^e_{h/c}}{1-p^e_{h/c}}\right)^{1/2}}{\left(\frac{1-p^e_{h/c}}{p^e_{h/c}}\right)^{1/2} + \left(\frac{p^e_{h/c}}{1-p^e_{h/c}}\right)^{1/2}} = (1-2p^e_{h/c}), \tag{4.7}$$

where $p^e_{h/c}$ are the populations of the excited state of the hot (h) and cold (c) reservoirs. Thus, we can rewrite the total work as

$$\langle W\rangle = -h(\nu_h - \nu_c)(p^+_h - p^+_c) + h\xi[\nu_c(1-2p^+_h) + \nu_h(1-2p^+_c)] \tag{4.8}$$

here, the work friction is

$$\langle W^{\text{fric}}\rangle = h\xi[\nu_c(1-2p^+_h) + \nu_h(1-2p^+_c)]. \tag{4.9}$$

We can also express the heat absorbed and released in terms of the populations of the excited state of both reservoirs

$$\langle Q_h\rangle = h\nu_h[p^+_h - p^+_c - \xi(1-2p^+_c)], \tag{4.10}$$

$$\langle Q_c\rangle = -h\nu_c[p^+_h - p^+_c - \xi(1-2p^+_h)]. \tag{4.11}$$

Note that Equation (4.9) allows us to create a map to analyze the region where it is possible to obtain friction work less than zero. Given the convention adopted in this work, this corresponds to friction work contributing as net work

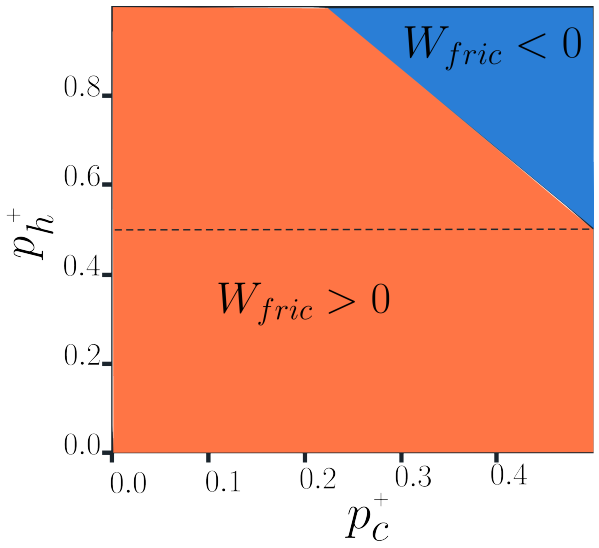

Figure 4.1: $W_{fric}\times$ populations. In the plot, we can observe that W^{fric}/ξ starts as positive (orange color) and becomes negative (blue color). The population p_h^+ varies from 0 to 1 , the dashed line represents when population inversion occurs, p_c^+ ranges from 0 to 0.5 and the frequencies are $\nu_h = 3.6kHz$ and $\nu_c = 2kHz$.

In Figure 4.1, we can observe the friction work as a function of the populations of the excited state for each reservoir. The choice of these populations determines the existence of negative friction work. We are considering that population inversion can only occur in the hot reservoir, so that the effective temperature is less than zero. This behavior is independent of the timing of the unitary transformations but depends on the choice of expansion (ν_h) and compression (ν_c) frequencies. We can observe this for values of p_h^+ that allow for $W_{fric} < 0$

$$p_h^+ > \frac{\nu_h}{\nu_c}\left(\frac{1}{2} - p_c^+\right) + \frac{1}{2}, \tag{4.12}$$

note that ν_h/ν_c determines the slope of the line that divides the region where there is negative friction work. The choice made for $\nu_h = 3.6kHz$ and $\nu_c = 2kHz$ is because they are the same values used in [35].

A simulation of the cycle was conducted using the Qutip library in Python. In this simulation, we considered that the hot reservoir was a fermionic reservoir with population inversion, and the dynamics of the system in that reservoir is described by Equation 3.53. We analyzed the behavior of the net work, heat, and efficiency by defining the populations of the excited state of the cold reservoir (p_c^+) with values corresponding to different regions of the map shown in Figure 4.1. All results were compared with the case where there was no population inversion in the hot reservoir.

4.1.1 Friction Work and Net Work

Considering initially the hot reservoir with $T > 0$, the population of the excited state of this reservoir was set to $p^+h = 0.45$. In the case where $T_{eff} < 0$, the chosen value for the hot reservoir was $p_h^+ = 0.8$. In both cases, the population in the cold reservoir (p_c^+) varies between 0.25, 0.30, 0.35, and 0.40, while the frequencies used are $\nu_h = 3.6kHz$ and $\nu_c = 2kHz$. Based on these settings, the graph below demonstrates the evolution of the net work obtained in the cycle as a function of time τ, during which the unitary transformations are performed

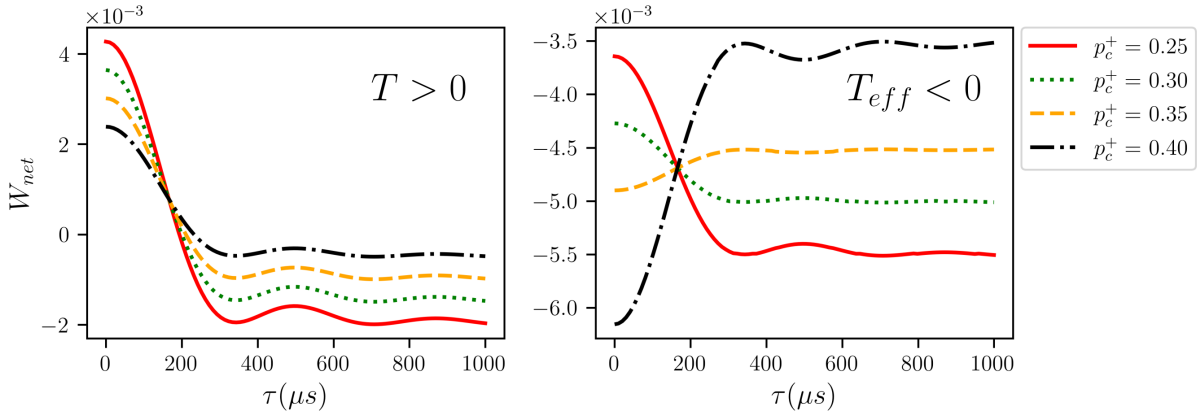

Figure 4.2: Behavior of Net Work as a Function of Time for Unitary Transformations. On the left, for $T > 0$, in the range $0 < \tau < 200$, there is no motor regime; on the right, when $T_{\text{eff}} < 0$, for all values of τ, there is a motor regime.

When $T > 0$, for $0 < \tau < 200$, the work done is positive ($W_{net} > 0$). In this scenario, internal friction is significant enough to prevent the existence of a engine regime. However, this situation differs when $T_{\text{eff}} < 0$, where, for all values of τ, the work done is negative ($W_{net} < 0$).

The choice for p_c^+ was made for different values, covering both those within and outside the regime where it is possible to obtain negative friction work in the case of population inversion. Using Equation 4.9, we have:

$$\frac{1}{2}\left(1 + (1 - 2p_h^+)\frac{\nu_c}{\nu_h}\right) < p_c^+ < \frac{1}{2}. \tag{4.13}$$

By fixing the value of $p_h^+ = 0.8$, Eq. 4.13 provides us with the interval for p_c^+ as $0.33 < p_c^+ < 0.5$. This characteristic, the existence of such a range where the friction work assumes negative values, holds significance as it implies that the friction work will be algebraically added in Eq. 4.8, resulting in an increase in the amount of useful work extracted. We can verify this in Figure 4.3

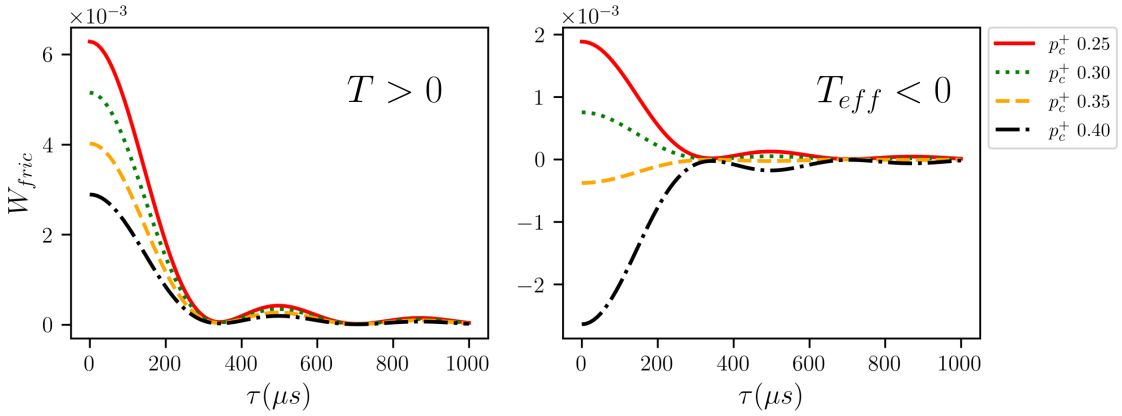

Figure 4.3: Friction work as a function of τ for $T > 0$ (on the left) and $T_{eff} < 0$ (on the right).

As the unitary transformations become faster, friction work increases. We can observe that by choosing the population p_c^+ within the interval $0.33 < p_c^+ < 0.5$, friction work takes on negative values, contributing favorably to the motor's performance.

Note that in the Figure 4.2 there is a crossover point between the curves where, at that specific time, it is possible to extract the same amount of net work, regardless of the value of p_c^+. The instant at which this occurs is solely determined by the frequencies of the expansion and compression strokes. This point can be obtained by taking the derivative of Equation 4.8 with respect to p_c^+, which gives

$$\frac{\partial \langle W \rangle}{\partial p_c^+} = h(\nu_h - \nu_c) - 2\xi\nu_h = 0, \tag{4.14}$$

$$\xi = \frac{1}{2} - \frac{\nu_c}{2\nu_h}. \tag{4.15}$$

4.1.2 Heat absorbed

In the regime of short times, it is observed that the heat absorbed decreases progressively. This occurs because, in the expansion stroke, the friction work, although positive and greater for short times, is subtracted from the heat absorbed during the quasi-static regime, as stated in Equation 4.10

$$\langle Q_h \rangle = \langle Q_h^{\text{ad}} \rangle - \langle W_{1\to 2}^{\text{fric}} \rangle, \tag{4.16}$$

where

$$\langle Q_h^{\text{ad}} \rangle = h\nu_h(1 - p_c^+ - p_h^+), \tag{4.17}$$

$$\langle W_{1\to 2}^{\text{fric}} \rangle = -\xi h\nu_h(1 - p_c^+). \tag{4.18}$$

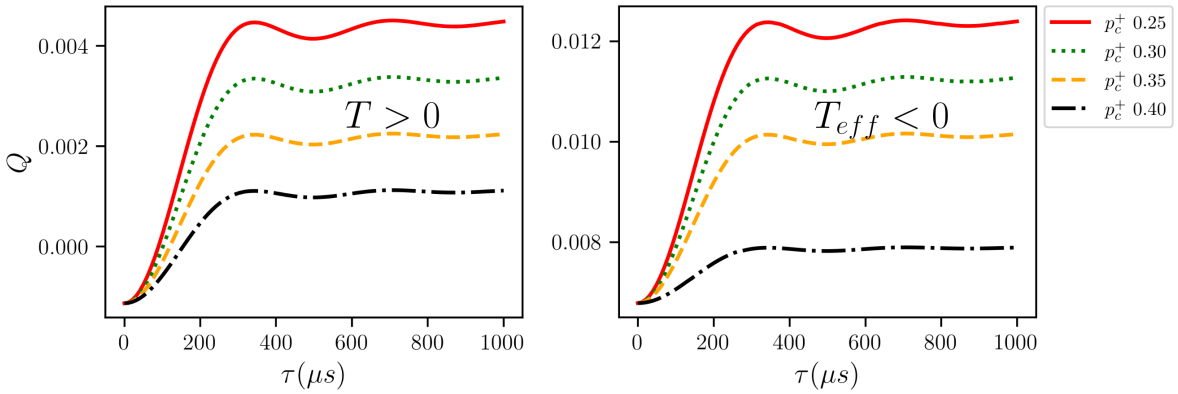

Figure 4.4: Heat as a function of τ for $T > 0$ and $T_{eff} < 0$.

It is evident from the Figure 4.4 that the heat decreases progressively for short time regimes. Furthermore, we can observe that the production of entropy leads to a decrease in the values assumed by heat for $T > 0$ also for $T_{eff} < 0$.

4.1.3 Efficiency

The study of work and heat is fundamental for evaluating the efficiency of the cycle in situations where the temperature (T) is greater than zero and when the effective temperature (T_{eff}) is less than zero. The cycle efficiency, represented by η, is calculated as the ratio between the average value of the work done and the average value of the heat absorbed, i.e., $\eta = -\langle W \rangle / \langle Q \rangle$. To visualize the behavior of this efficiency in different scenarios, the figure below illustrates the variations over different times of unitary transformations.

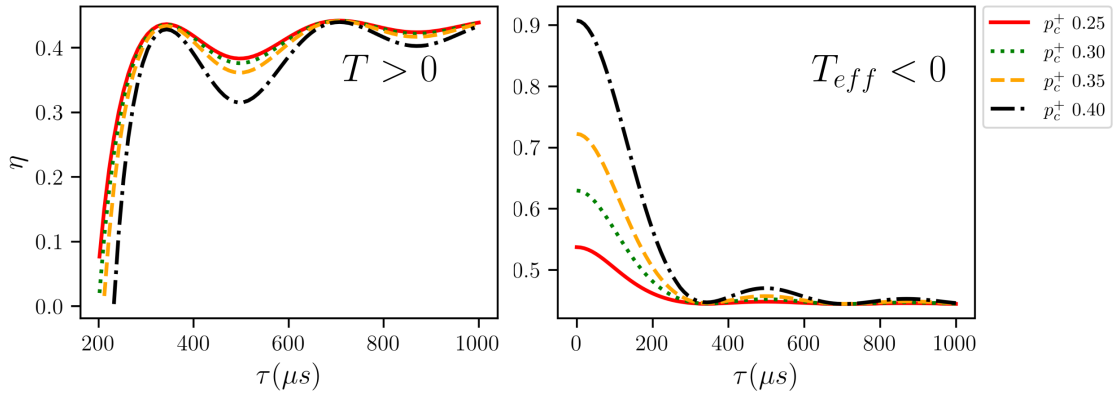

Figure 4.5: Efficiency for $T < 0$. It can be observed that efficiency takes higher values within the determined interval, $0.33 < p_c^+ < 0.5$, for shorter times.

Comparing the efficiency in the two temperature regimes, it is noticeable that, at finite times, the efficiency is higher for negative temperatures due to two reasons: Firstly, with the appropriate choice of population, where $W^{\text{fric}} < 0$, it becomes possible to obtain a

higher value for $|W|$, resulting in an additional increase in efficiency. Additionally, in both reservoirs, the term associated with the finite-time regime reduces the amount of absorbed heat. However, in the case where $T > 0$, friction work is so significant at short times that it deteriorates the system's efficiency. On the other hand, in the scenario of $T_{\text{eff}} < 0$, the work done is more substantial at short times, which, in turn, enhances efficiency. It is important to note that, in both cases, as the parameter τ approaches large values, i.e., in the quasi-static regime, both efficiencies tend to approach the Otto efficiency, which, as expressed in the Equation 3.90, depends exclusively on the frequencies.

4.2 Thermodynamic Properties of a Single Qubit and the Nernst Theorem

As we discussed in Chapter 2, the Nernst Heat Theorem is commonly treated as a postulate due to a lack of demonstration or robust experimental verifications. In order to investigate this theorem more deeply, we extended the concepts related to thermodynamic potentials to the quantum scale, applying them to a single qubit. Additionally, we analyzed the behavior of the thermal capacity and entropy of this single qubit under low-temperature conditions. To conduct this analysis, we used the scheme depicted in Figure 4.6 in our simulations and experiments

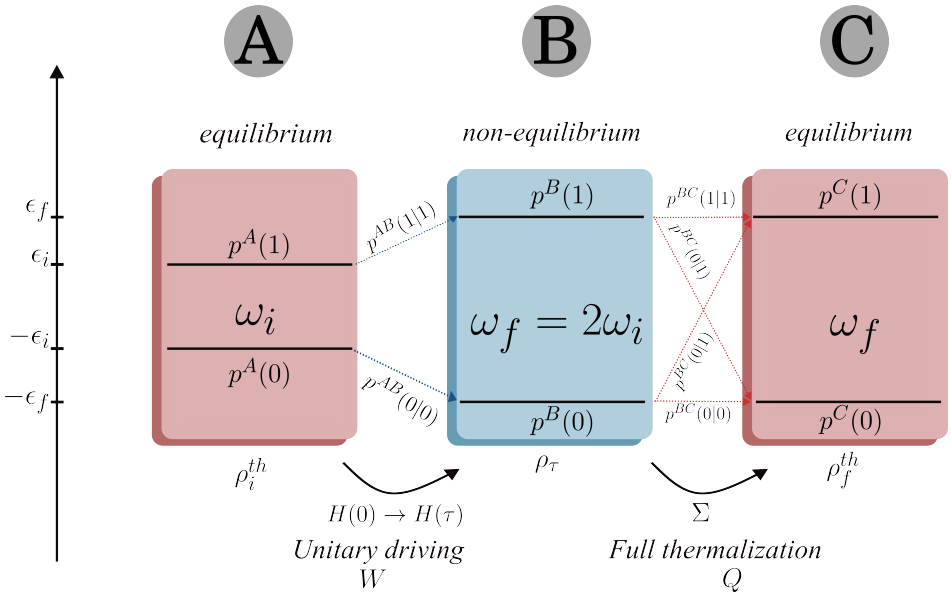

Figure 4.6: Schematic diagram of the process conducted in a two-level system. From A to B, there is a unitary expansion of the energy gap. In the B to C stage, the Hamiltonian remains constant, and the system undergoes thermalization with the reservoir.

Considering a two-level system whose Hamiltonian is expressed by

$$H = \frac{h\nu}{2}\sigma_z, \tag{4.19}$$

and that this system is in contact with a reservoir at a fixed temperature T, being in a state of thermal equilibrium.

$$\rho = \frac{e^{-\beta H}}{2\cosh\frac{\beta h\nu}{2}} \tag{4.20}$$

with the partition function $Z = 2\cosh\frac{\beta h\nu}{2}$.The internal energy U of the system is given by

$$U = \mathrm{Tr}\{\rho H\} = -\frac{h\nu}{2}\tanh\frac{\beta h\nu}{2}, \tag{4.21}$$

we can calculate the entropy as

$$\begin{aligned} S &= -k_b\,\mathrm{Tr}\{\rho\ln\rho\} = -k_b(p_e\ln p_e + p_g\ln p_g) \\ &= \frac{-k_b}{2\cosh\frac{\beta h\nu}{2}}e^{-\beta\hbar\omega/2}\left(\ln e^{-\frac{\beta h\nu}{2}} - \ln 2\cosh\frac{\beta h\nu}{2}\right) \\ &+ \frac{-k_b}{2\cosh\frac{\beta h\nu}{2}}e^{\beta\hbar\omega/2}\left(\ln e^{\frac{\beta h\nu}{2}} - \ln 2\cosh\frac{\beta h\nu}{2}\right) \\ &= -k_b\frac{\beta h\nu}{2}\tanh\frac{\beta h\nu}{2} + k_b\ln\cosh\frac{\beta h\nu}{2} + k_b\ln 2. \end{aligned} \tag{4.22}$$

The process consists of two steps. Initially, the system starts from a state of thermal equilibrium ρ_i^{th} and in the transition from A to B, there is a unitary expansion in the energy gap with no variation in entropy. This results in a non-equilibrium state ρ_τ^{neq} at the end of the expansion. Subsequently, in the transition from B to C, the system undergoes a thermalization process with the reservoir, reaching a state of equilibrium ρ_f^{eq}, During the thermalization process, entropy production occurs.

According to the laws of thermodynamics, the change in internal energy of a system corresponds to the sum of the work done on or by the system and the heat released or absorbed in the process. We can express this relationship as follows: $\Delta U = \langle W\rangle + \langle Q\rangle$. The work done in this process occurs during the unitary expansion stage, and the expected value of this work is given by:

$$\langle W\rangle = \mathrm{Tr}\{\rho_i(H_f - H_i)\}, \tag{4.23}$$

with H_i and H_f being the Hamiltonians at the beginning and at the end of the expansion stroke, respectively. Heat occurs during the thermalization stroke, represented by

$$\langle Q\rangle = k_B T(\Delta S_{vN} - \langle\Sigma\rangle), \tag{4.24}$$

In which T is the temperature of the reservoir, ΔS_{vN} is the von Neumann entropy change for the states ρ_f and ρ_i, and $\langle\Sigma\rangle$ corresponds to the entropy production. The difference

between ΔS_{vN} and $\langle\Sigma\rangle$ represents the exchange[a] of entropy between the system and the reservoir.

To determine whether the cooling protocol is in accordance with the third law as proposed by Nernst's heat theorem, we will take an approach based on the entropy production at low temperatures, which we will call the static approach, alternatively to the dynamic approach taken by Kosloff et al. [26] as discussed in Section 3.3. Based on the behavior of heat in relation to temperature and considering the Equation 4.24, we can express the production of entropy from step B to C as:

$$\langle\Sigma\rangle = \beta(\Delta S_{vN} - \langle Q\rangle). \tag{4.25}$$

According to Nernst's theorem, as the temperature approaches zero, the entropy change becomes zero. This implies that:

$$\langle\Sigma\rangle \approx -\beta \langle Q\rangle , \tag{4.26}$$

given our protocol, at this stage, heat corresponds to the energy extracted from the system, which, due to the adopted convention, has a negative sign. Therefore since the second law implies that $\Sigma \geq 0$, we have

$$\langle\Sigma\rangle \approx \left|\frac{\langle Q\rangle}{\kappa_B T}\right| \geq 0. \tag{4.27}$$

Entropy production is calculated between the thermal equilibrium states at the beginning and end of the protocol, both represented by diagonal states on the same basis, resulting in a finite quantity. As the temperature T approaches zero, the average heat $\langle Q\rangle$ must be proportional to a power of the temperature, expressed by:

$$\langle Q\rangle \propto T^{\alpha}, \tag{4.28}$$

where $\alpha \geq 1$, so $\langle\Sigma\rangle$ remains finite.

4.2.1 Quantum Analogues of Thermodynamic Potentials

The Helmholtz free energy tells us the maximum amount of work that can be extracted from a system under constant temperature. The change in this energy can be

a. Note that Equation 4.24 is the analogue of Equation 3.60. To see this, simply multiply both sides of Equation 3.60 by T.

expressed as follows:

$$\Delta F = \Delta U - T\Delta S, \tag{4.29}$$

substituting $\Delta U = \mathrm{Tr}\{H_f\rho_f - H_i\rho_i\}$, we have:

$$\Delta F = \mathrm{Tr}\{\rho_i(H_f - H_i)\} - T\langle\Sigma\rangle = \mathrm{Tr}\{\rho_i(H_f - H_i)\} - k_BT(-\mathrm{Tr}\{\rho_i \ln\rho_f\} - \mathrm{Tr}\{\rho_i\ln\rho_i\}),$$

simplifying this expression:

$$\Delta F = -\frac{1}{\beta}\ln\frac{Z(\beta,\nu_f)}{Z(\beta,\nu_i)}. \tag{4.30}$$

This is nothing more than the difference between the average work $\langle W\rangle$ and the dissipated work W_d

$$W_d = T\langle\Sigma\rangle. \tag{4.31}$$

Which, in this case, corresponds to the work lost due to the production of residual entropy. In the classical context, enthalpy in a process at constant pressure corresponds to the heat absorbed or released in the process

$$\Delta H = \Delta U + P\Delta V = \Delta U - \langle W\rangle = \langle Q\rangle. \tag{4.32}$$

Let's consider an analogous potential that corresponds only to the heat absorbed

$$\Delta\mathcal{H} = T\Delta S - k_BT(-\mathrm{Tr}\{\rho_i\ln\rho_f\} - \mathrm{Tr}\{\rho_i\ln\rho_i\}) = T\Delta S - k_BTD(\rho_i||\rho_f). \tag{4.33}$$

Note that $\mathrm{Tr}\{\rho_i\ln\rho_f\} = -\mathrm{Tr}\{\rho_iH_f\}\beta - \ln Z(\beta,\nu_f)$, so

$$\Delta\mathcal{H} = \mathrm{Tr}\{\rho_fH_f\} + \frac{1}{\beta}\ln Z(\beta,\nu_f) - \mathrm{Tr}\{\rho_iH_f\} - \frac{1}{\beta}\ln Z(\beta,\nu_f),$$

therefore

$$\Delta\mathcal{H} = \mathrm{Tr}\{(\rho_f - \rho_i)H_f\}. \tag{4.34}$$

The Gibbs free energy, represented by G, is defined as the difference between enthalpy H and the product of temperature T and entropy S, with the variation of G keeping T constant given by:

$$\Delta G = \Delta H - T\Delta S. \tag{4.35}$$

Now let us consider the existence of an analogous potential $\mathcal{G}$, whose variation corresponds to

$$\Delta\mathcal{G} = \Delta\mathcal{H} - T\Delta S, \tag{4.36}$$

so

$$\Delta\mathcal{G} = \mathrm{Tr}\{(\rho_f - \rho_i)H_f\} - T\Delta S$$

$$\Delta\mathcal{G} = -\frac{1}{\beta}D(\rho_i||\rho_f). \tag{4.37}$$

Note that all the potentials presented so far depend exclusively on the initial and final equilibrium states, as well as their respective Hamiltonians, as outlined in the table below:

ΔU	$\mathrm{Tr}\{\rho_f H_f\} - \mathrm{Tr}\{\rho_i H_i\}$
ΔF	$-k_b T \ln \frac{Z(\beta,\nu_f)}{Z(\beta,\nu_i)}$
$\Delta\mathcal{H}$	$\mathrm{Tr}\{(\rho_f - \rho_i)H_f\}$
$\Delta\mathcal{G}$	$-\frac{1}{\beta}D(\rho_i\|\|\rho_f)$

Table 4.1: Quantum Analogues of Thermodynamic Potentials

4.2.2 Response function as an Analogue to Heat Capacity

In the classical context, heat capacity refers to the amount of heat absorbed or released to allow a change in the system's temperature. This relationship can be expressed mathematically as follows:

$$C = \frac{Q}{\Delta T}. \tag{4.38}$$

As mentioned earlier, both the initial and final states of the process have the same temperature, even if there is a heat exchange $\langle Q\rangle$, the difference $\Delta T = 0$. However, if we focus exclusively on the stage where heat transfer occurs, namely, during the thermalization stage ($\rho_\tau \to \rho_f$), it is possible to assign an effective temperature to the state ρ_τ since the state ρ_τ is diagonal

$$\rho_\tau = \frac{e^{-\beta_{eff}H_f}}{Z(\beta_{eff},\nu_f)}. \tag{4.39}$$

The expansion of the gap defining the first stage ($\rho_i \to \rho_\tau$) occurs unitarily. This means that the probabilities p_i^e and p_i^g become equal to the probabilities p_τ^e and p_τ^g, respectively. From the relation $p_i^e/p_i^g = e^{-\beta\nu_i}$, we can establish a connection between the effective temperature and the equilibrium temperature:

$$e^{-\beta\nu_i} = e^{-\beta_{eff}\nu_f}, \tag{4.40}$$

that is

$$T_{eff} = \frac{\nu_f}{\nu_i}T. \tag{4.41}$$

Note that this effective temperature is higher than the equilibrium temperature because $\nu_f > \nu_i$. Thus, we can define a response function $\mathcal{C}$, which corresponds to the

heat absorbed or released for a given temperature change $\Delta T_\tau = T - T_{eff}$

$$\mathcal{C} = \frac{\langle Q \rangle}{\Delta T_\tau}, \qquad \Delta T_\tau = \left(1 - \frac{\nu_f}{\nu_i}\right) T. \tag{4.42}$$

4.2.3 QuTiP Simulation

Utilizing the open-source QuTiP library in Python, we can perform simulations of quantum systems, both closed and open. In this context, simulating an expansion process is described by a time-dependent Hamiltonian

$$H(t) = \frac{h}{2}((\nu_f - \nu_i)t/\tau - \nu_i)\sigma_z, \tag{4.43}$$

in which τ represents the final time of the expansion, and $t = [0, \tau]$. During thermalization, the system's dynamics are governed by the master equation, where $\rho(0) = \rho_\tau$ and ρ_f is the asymptotic state.

For different reservoir temperatures, all stages were simulated, allowing us to obtain graphs representing analogs to thermodynamic potentials as shown in Figure 4.7.

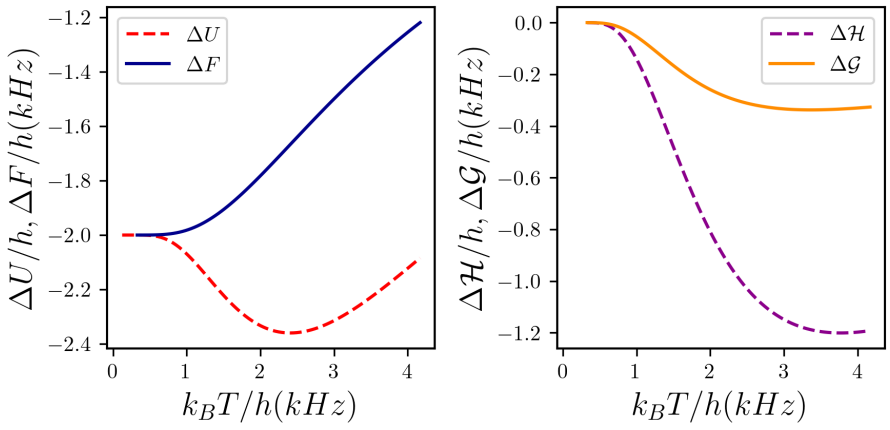

Figure 4.7: Simulation of the behavior of the functions ΔU, ΔF, $\Delta\mathcal{H}$ and $\Delta\mathcal{G}$ for a single qubit in the low-temperature limit.

Note that the same behavior indicated by Nernst (see Figure 2.1a) is also observed in a single qubit, where energies tend to a minimum value as temperature decreases. This suggests that thermodynamic characteristics are preserved in this quantum context.

Figure 4.8 shows the behavior of von Neumann entropy and entropy production in the same limit, both converging to zero. The negative variation of von Neumann entropy can be justified by the fact that, during the thermalization stroke, the system releases heat. On the other hand, entropy production remains always positive, in accordance with Equation 3.75

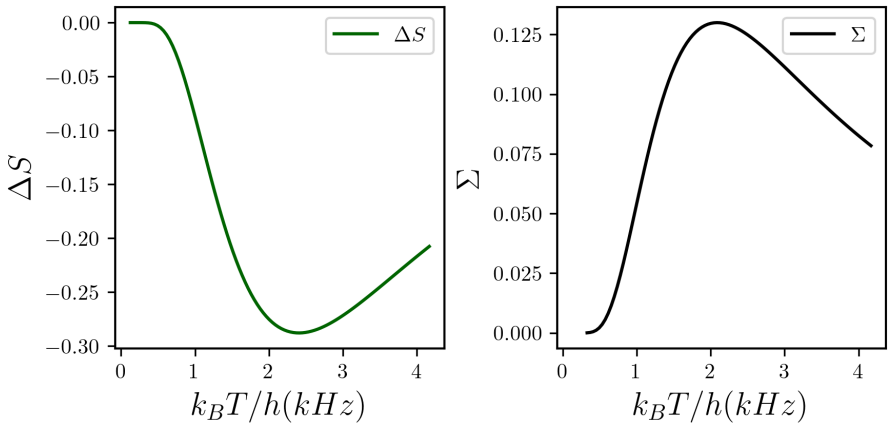

Figure 4.8: Variation of von Neumann Entropy (ΔS) and Entropy Production (Σ) as a function of Temperature

The graph presented in Figure 4.9 shows the response function, Equation 4.42, which is our analogue to heat capacity, for different equilibrium temperatures.

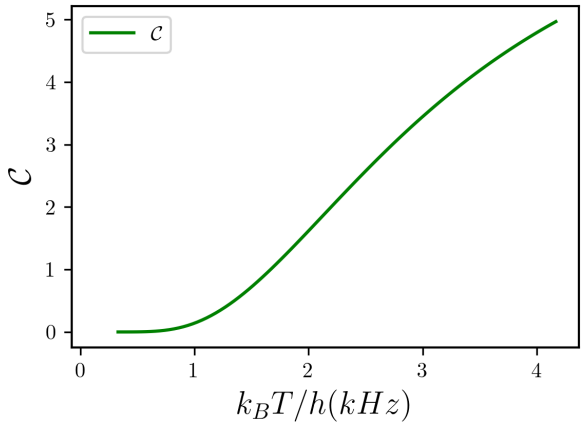

Figure 4.9: Response function $\mathcal{C}$ for different temperatures.

This analogue to heat capacity also tends to zero in the low-temperature limit, as it occurs in the classical case.

As mentioned at the beginning of this section, in extremely low temperature conditions, heat must behave as a temperature power, as presented in Equation 4.28. Considering that the entropy change ΔS tends to zero in this limit, we can analyze this behavior by fitting the heat curve Q, obtained through simulation, by a function $f(T) = aT^{\alpha}$. The results obtained were $a = -0.17$ and $\alpha = 2.30$, as illustrated in Figure 4.10.

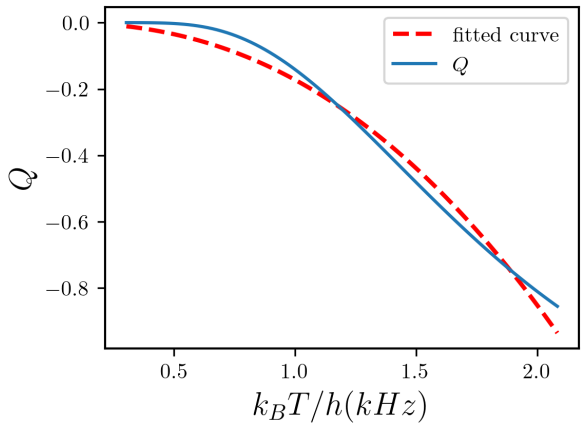

Figure 4.10: Q as a Function of Temperature and the fitted curve where $f(T) = -0.17T^{2.30}$.

Note that the value of α found is greater than one, which complies with the restriction established by the third law.

4.2.4 Experimental Results

In addition to numerical simulation, an experiment was also conducted using the Nuclear Magnetic Resonance (NMR) technique. In the context of quantum information, the nuclear spins of atoms in the sample are used as qubit.The experiment was conducted in collaboration with researchers from UFABC, and the results presented below were also included in [3]. The general concepts of the technique can be found in Appendix B, while details on how it was implemented for this context will be presented in [3].

In the experiment, a sample of 13 C-labelled trichloromethane ($CHCl_3$) diluted in d-acetone (C_3D_6O) was used. The tomography of the obtained state allows extracting various thermodynamic information. For example, the temperature can be obtained by

$$T = \frac{2\Delta E}{k_b} \ln \frac{p^+}{1-p^+}, \tag{4.44}$$

heat and work can be obtained through the first law, based on the system's energy variation, as it is well defined in each stage when work and heat occur. Another way to obtain heat and work is through the magnetization along the z-axis

$$\langle W \rangle = \langle \mathcal{M}_z \rangle_B - \langle \mathcal{M}_z \rangle_A \tag{4.45}$$

$$\langle Q \rangle = \langle \mathcal{M}_z \rangle_C - \langle \mathcal{M}_z \rangle_B \tag{4.46}$$

The fluctuation-dissipation theorem and the Jarzinski equality allow finding ΔF, and the entropy change is obtained using von Neumann entropy.

In Figure 4.11, we can observe that the released heat approaches zero as the temperature tends to zero. On the other hand, the work tends towards the same value as the minimum internal energy. In view of the first law of thermodynamics, this behavior is expected

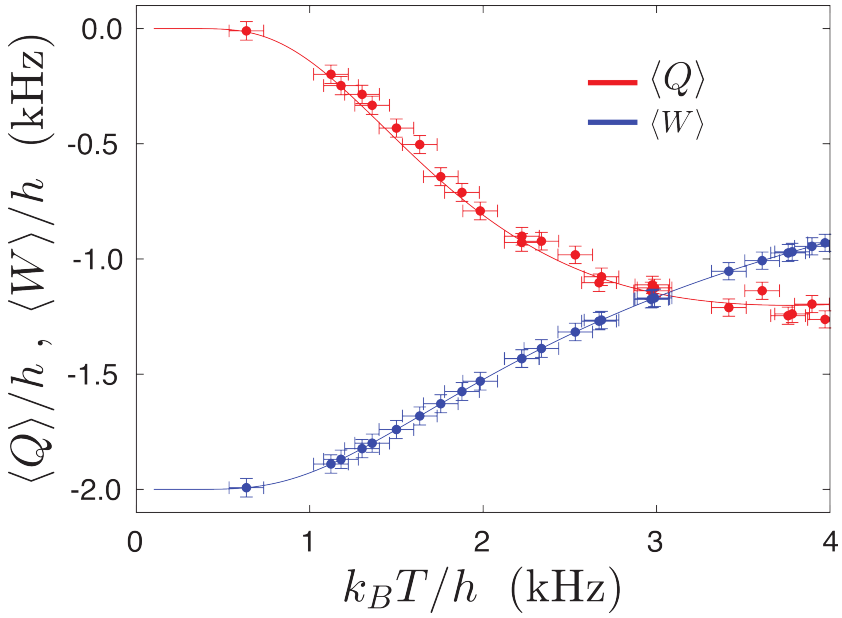

Figure 4.11: Experimental Results of Heat and Work for Different Temperatures [3].

The entropy change in this process is negative because the system releases heat during the process, approaching zero as the reservoir temperature approaches zero, as shown in Figure 4.12

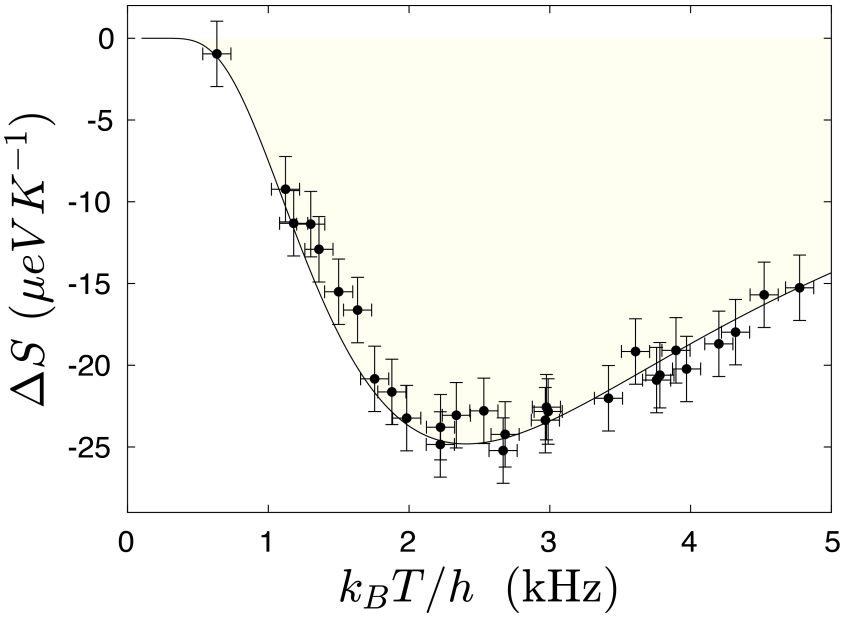

Figure 4.12: Experimental Values of Entropy Change and Work for Different Temperatures [3].

Figures 4.13 and 4.14 present the results obtained in the experiment for the Helmholtz free energy and internal energy. In the first image, it corresponds to the range of k_BT/h between 0 and 5 kHz, while in Figure 4.14, the corresponding range is k_BT/h between 0 and 2 kHz. It is observed that the points converge to the same value in the limit as the temperature approaches zero

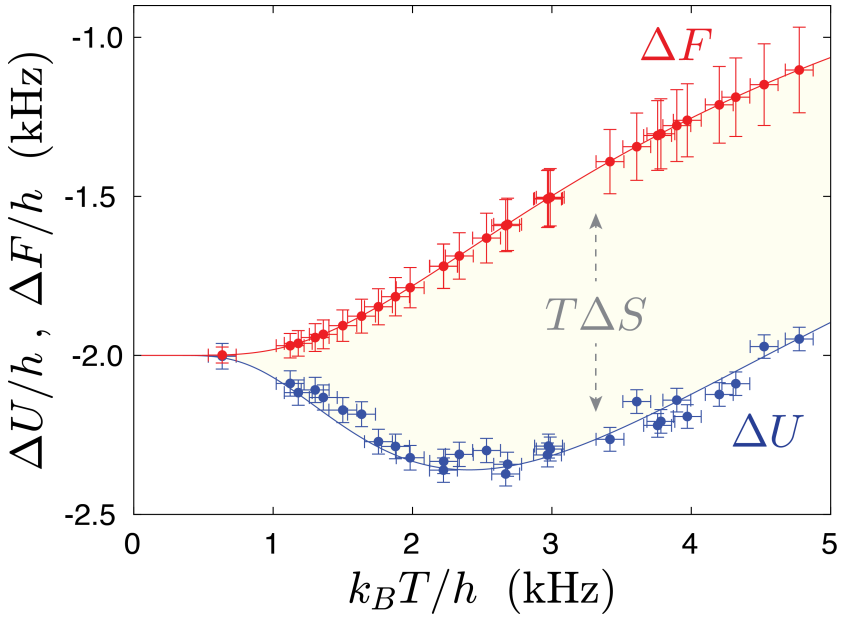

Figure 4.13: Experimental Points ΔF and ΔU as a Function of Temperature [3].

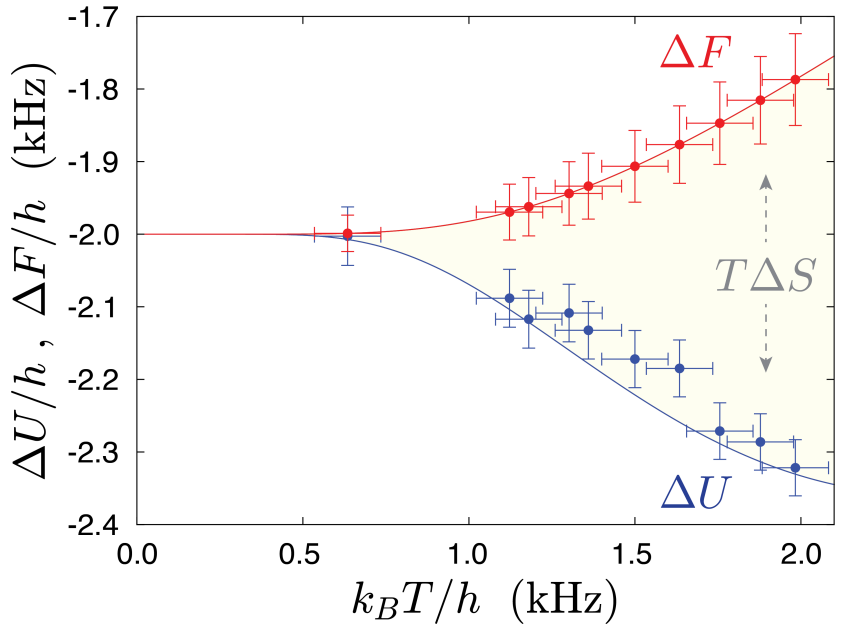

Figure 4.14: Experimental Points ΔF and ΔU as a Function of Temperature whit k_BT/h between 0 and 2 kHz [3].

It can be noted that the values of ΔF and ΔU exhibit the same behavior that Nernst stated in [14]. On a fundamental scale, such as that of a single qubit, we can observe

not only the behavior of heat, work, and entropy for systems at such low temperatures but also elucidate the ideas proposed by Nernst in his heat theorem.

Analyzing the behavior of heat in the limit of low temperatures, it is possible to observe that the experimental points in Figure 4.15 are well adjusted by:

$$f(k_BT) = 6.3(e^{-\frac{8.2}{k_BTh}} - e^{-\frac{3.9\hbar}{k_BT}}), \tag{4.47}$$

represented by the red dotted line. When assigning behavior like $aT^{-\alpha}$, we obtain the black dashed curve, as expressed in the equation below:

$$Q_{fit}(T) = -\frac{T^{8/5}}{4}. \tag{4.48}$$

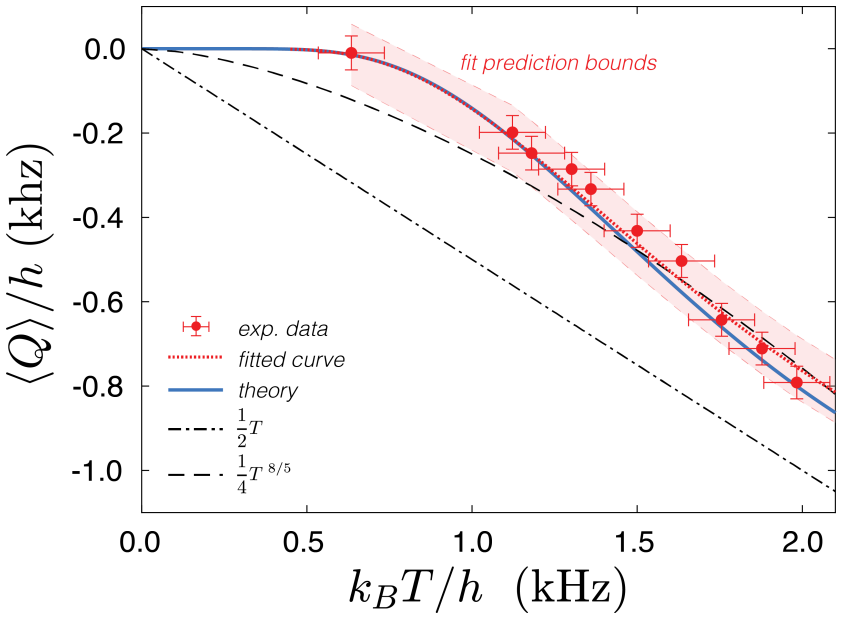

Figure 4.15: Experimental Points Q as a Function of Temperature with k_BT/h between 0 and 2 kHz.

The value of $\alpha = 8/5$ is in agreement with the simulation result, since both are greater than one. Considering the restriction of the third law ($\alpha \geq 1$), the line composed of dots and dashes represents the limit situation, in which $\alpha = 1$. Although the heat extraction protocol complies with the third law, it is not optimized to reach its limit, leaving this question open.

CHAPTER 5

Conclusions

In this monograph, we presented the theoretical framework necessary to understand the emergence of entropy production in quantum systems and its impact on quantum thermal machines. By addressing quantum friction, i.e., the probability transitions between states occurring in unitary evolutions, we highlighted how these phenomena can compromise the performance of a quantum Otto cycle. Furthermore, by considering the laws of thermodynamics on a fundamental scale, we were able to observe a process that enables an analysis of Nernst's heat theorem for a single qubit.

Thus far, we have highlighted as a result the fact that operating the QOHE with one of the reservoirs exhibiting population inversion, can explain the increase in efficiency. This improvement arises from the strategic choice of populations in the excited states of the reservoirs, allowing for negative friction work. We demonstrated that for this specific engine, there are conditions in which an increase in internal friction leads to higher useful work, resulting not only in higher efficiency but also in a gain in power. This is because internal friction is greater when the expansion and compression processes occur in short times

Another relevant result we addressed is the extension of Nernst's heat theorem to a single qubit. This theorem has sparked various discussions, as, until now, there are no conclusive proofs. However, through a theoretical approach, numerical simulations, and experiments using NMR, we were able to demonstrate that the Helmholtz free energy and internal energy converge to the same value as we approach zero Kelvin, as stated by Nernst. We also demonstrate the extension of the idea presented in [26] about the cooling rate in relation to the third law, where $Q \propto T^{\alpha}$, when Q is the extracted heat during the cooling process and T is the temperature at the end of the process in the limit of low temperatures. When analyzing only the heat extracted in the process, we obtained of $\alpha > 1$ thus confirming that this heat extraction protocol is in accordance with the third law.

It is important to highlight that the system under consideration consists of a single qubit. The application of this protocol for heat extraction exclusively involves gap

expansion and thermalization, resulting in the production of entropy through "residual lag", without the presence of quantum friction. When observing the limits of low temperatures, we notice that our potentials, equivalent to classical thermodynamic potentials, follow the behavior predicted by Nernst. In this same limit, entropy tends to a constant value, while heat behaves as a power of temperature, with $\alpha = 2.3$. These results lead us to the conclusion that, for this quantum system and this specific protocol, Nernst's heat theorem remains valid.

Bibliography

[1] RAMSEY, N. F. Thermodynamics and statistical mechanics at negative absolute temperatures. **Phys. Rev.**, American Physical Society, v. 103, p. 20–28, Jul 1956. Disponível em: <https://link.aps.org/doi/10.1103/PhysRev.103.20>. Cited 4 times on pages xii e 11

[2] r, M. Koláet al. Quantum bath refrigeration towards absolute zero: Challenging the unattainability principle. **Phys. Rev. Lett.**, American Physical Society, v. 109, p. 090601, Aug 2012. Disponível em: <https://link.aps.org/doi/10.1103/PhysRevLett.109.090601>. Cited 3 times on pages xii, 22 e 23

[3] VIEIRA, C. H. S. **INVESTIGAÇÕES EXPERIMENTAIS SOBRE FLUTUAÇÕES, INCERTEZAS E LIMITES EM TERMODINÂMICA QUÂNTICA**. 150 f. Tese (Doutorado em Física) — PÓS-GRADUAÇÃO EM FÍSICA, Universidade Federal do ABC, Santo André, 2023. Cited 10 times on pages xiii, 46, 47 e 48

[4] CARDWELL, D. **From Watt to Clausius: The Rise of Thermodynamics in the Early Industrial Age**. Cornell University Press, 1971. ISBN 9780801406782. Disponível em: <https://books.google.com.br/books?id=NJEyAAAAMAAJ>. Cited 3 times on pages 1 e 3

[5] MAHLER, G.; GEMMER, J.; MICHEL, M. Emergence of thermodynamic behavior within composite quantum systems. **Physica E: Low-dimensional Systems and Nanostructures**, Elsevier BV, v. 29, n. 1–2, p. 53–65, out. 2005. ISSN 1386-9477. Disponível em: <http://dx.doi.org/10.1016/j.physe.2005.05.001>. Cited on page 1.

[6] PLASTINA, F. et al. Irreversible work and inner friction in quantum thermodynamic processes. **Phys. Rev. Lett.**, American Physical Society, v. 113, p. 260601, Dec 2014. Disponível em: <https://link.aps.org/doi/10.1103/PhysRevLett.113.260601>. Cited 5 times on pages 1, 22, 29 e 30

[7] MEHBOUDI, M.; SANPERA, A.; CORREA, L. A. Thermometry in the quantum regime: recent theoretical progress. **Journal of Physics A: Mathematical and Theoretical**, IOP Publishing, v. 52, n. 30, p. 303001, jul 2019. Disponível em: <https://dx.doi.org/10.1088/1751-8121/ab2828>. Cited on page 2.

[8] BUFFONI, L. et al. Third law of thermodynamics and the scaling of quantum computers. **Phys. Rev. Lett.**, American Physical Society, v. 129, p. 150602, Oct 2022. Disponível em: <https://link.aps.org/doi/10.1103/PhysRevLett.129.150602>. Cited 2 times on pages 2 e 22

[9] KIEU, T. D. Principle of unattainability of absolute zero temperature, the third law of thermodynamics, and projective quantum measurements. **Physics Letters A**, v. 383, n. 27, p. 125848, 2019. ISSN 0375-9601. Disponível em: <https://www.sciencedirect.com/science/article/pii/S037596011930636X>. Cited 2 times on pages 2 e 22

[10] ASSIS R. J.; SOUSA, A. F. et al. Power of a quantum otto heat engine operating under a reservoir at effective negative temperatures. **Manuscript in Production**. Cited on page 2.

[11] SOUSA A. F. ; VIEIRA, C. H. S. et al. Experimental investigation of nernst heat theorem and the third law of thermodynamicsat quantum scale. **Manuscript in Production**. Cited on page 2.

[12] CALLEN, H. B. **Thermodynamics and an introduction to thermostatistics; 2nd ed.** New York, NY: Wiley, 1985. Disponível em: <https://cds.cern.ch/record/450289>. Cited 6 times on pages 5, 6 e 9

[13] CARDWELL, D. S. L. **From Watt to Clausius: The Rise of Thermodynamics in the Early Industrial Age**. New York, NY: Cornell, 1971. Disponível em: <https://cds.cern.ch/record/450289>. Cited on page 5.

[14] NERSNT, W. **The New Theory of Heat**. New York, NY: Methuen and Company,, 1926. Cited 4 times on pages 5, 6 e 48

[15] KOX, A. Confusion and clarification: Albert einstein and walther nernst's heat theorem, 1911–1916. **Studies in History and Philosophy of Science Part B: Studies in History and Philosophy of Modern Physics**, v. 37, n. 1, p. 101–114, 2006. ISSN 1355-2198. 2005: The Centenary of Einstein's Annus Mirabilis. Disponível em: <https://www.sciencedirect.com/science/article/pii/S1355219805000687>. Cited 5 times on pages 6, 7 e 23

[16] DEBENEDETTI, P. G.; STILLINGER, F. H. Supercooled liquids and the glass transition. **Nature**, v. 410, n. 6825, p. 259–267, Mar 2001. ISSN 1476-4687. Disponível em: <https://doi.org/10.1038/35065704>. Cited on page 6.

[17] PURCELL, E. M.; POUND, R. V. A nuclear spin system at negative temperature. **Phys. Rev.**, American Physical Society, v. 81, p. 279–280, Jan 1951. Disponível em: <https://link.aps.org/doi/10.1103/PhysRev.81.279>. Cited 3 times on pages 10 e 19

[18] CARMICHAEL, H. J.; SCULLY, M. O. Statistical Methods in Quantum Optics 1: Master Equations and Fokker-Planck Equations. **Physics Today**, v. 53, n. 3, p. 78–80, 03 2000. ISSN 0031-9228. Disponível em: <https://doi.org/10.1063/1.883009>. Cited on page 14.

[19] BREUER, H.-P.; PETRUCCIONE, F. **The Theory of Open Quantum Systems**. Oxford University Press, 2007. ISBN 9780199213900. Disponível em: <https://doi.org/10.1093/acprof:oso/9780199213900.001.0001>. Cited on page 15.

[20] BAMBA, M.; IMOTO, N. Maxwell boundary conditions imply non-lindblad master equation. **Phys. Rev. A**, American Physical Society, v. 94, p. 033802, Sep 2016. Disponível em: <https://link.aps.org/doi/10.1103/PhysRevA.94.033802>. Cited on page 19.

[21] GHOSH, A.; SINHA, S. S.; RAY, D. S. Fermionic oscillator in a fermionic bath. **Phys. Rev. E**, American Physical Society, v. 86, p. 011138, Jul 2012. Disponível em: <https://link.aps.org/doi/10.1103/PhysRevE.86.011138>. Cited on page 19.

[22] ALICKI, R. The quantum open system as a model of the heat engine. **Journal of Physics A: Mathematical and General**, v. 12, n. 5, p. L103, may 1979. Disponível em: <https://dx.doi.org/10.1088/0305-4470/12/5/007>. Cited on page 20.

[23] GREINER, W.; NEISE, L.; STÖCKER, H. **Thermodynamics and Statistical Mechanics**. Springer-Verlag, 1995. (Classical theoretical physics). ISBN 9780387942995. Disponível em: <https://books.google.com.br/books?id=V6zvAAAAMAAJ>. Cited on page 20.

[24] MOHAMMADY, M. H.; MIYADERA, T. Quantum measurements constrained by the third law of thermodynamics. **Phys. Rev. A**, American Physical Society, v. 107, p. 022406, Feb 2023. Disponível em: <https://link.aps.org/doi/10.1103/PhysRevA.107.022406>. Cited on page 22.

[25] MASANES, L.; OPPENHEIM, J. A general derivation and quantification of the third law of thermodynamics. **Nature Communications**, v. 8, n. 1, p. 14538, Mar 2017. ISSN 2041-1723. Disponível em: <https://doi.org/10.1038/ncomms14538>. Cited on page 23.

[26] LEVY, A.; ALICKI, R.; KOSLOFF, R. Quantum refrigerators and the third law of thermodynamics. **Phys. Rev. E**, American Physical Society, v. 85, p. 061126, Jun 2012. Disponível em: <https://link.aps.org/doi/10.1103/PhysRevE.85.061126>. Cited 3 times on pages 23, 41 e 50

[27] QUAN, H. T. et al. Quantum thermodynamic cycles and quantum heat engines. **Phys. Rev. E**, American Physical Society, v. 76, p. 031105, Sep 2007. Disponível em: <https://link.aps.org/doi/10.1103/PhysRevE.76.031105>. Cited on page 25.

[28] PETERSON, J. P. S. et al. Experimental characterization of a spin quantum heat engine. **Phys. Rev. Lett.**, American Physical Society, v. 123, p. 240601, Dec 2019. Disponível em: <https://link.aps.org/doi/10.1103/PhysRevLett.123.240601>. Cited on page 25.

[29] CROOKS, G. E. Entropy production fluctuation theorem and the nonequilibrium work relation for free energy differences. **Phys. Rev. E**, American Physical Society, v. 60, p. 2721–2726, Sep 1999. Disponível em: <https://link.aps.org/doi/10.1103/PhysRevE.60.2721>. Cited on page 26.

[30] TALKNER, P.; HäNGGI, P. The tasaki–crooks quantum fluctuation theorem. **Journal of Physics A: Mathematical and Theoretical**, v. 40, n. 26, p. F569, jun 2007. Disponível em: <https://dx.doi.org/10.1088/1751-8113/40/26/F08>. Cited on page 26.

[31] AO, T. B. B. et al. Experimental reconstruction of work distribution and study of fluctuation relations in a closed quantum system. **Phys. Rev. Lett.**, American Physical Society, v. 113, p. 140601, Oct 2014. Disponível em: <https://link.aps.org/doi/10.1103/PhysRevLett.113.140601>. Cited on page 27.

[32] CAMPISI, M.; HÄNGGI, P.; TALKNER, P. Colloquium: Quantum fluctuation relations: Foundations and applications. **Rev. Mod. Phys.**, American Physical Society, v. 83, p. 771–791, Jul 2011. Disponível em: <https://link.aps.org/doi/10.1103/RevModPhys.83.771>. Cited 3 times on pages 27 e 28

[33] JENSEN, J. L. W. V. Sur les fonctions convexes et les inégalités entre les valeurs moyennes. **Acta mathematica**, Springer, v. 30, n. 1, p. 175–193, 1906. Cited on page 29.

[34] LANDI, G. T.; PATERNOSTRO, M. Irreversible entropy production: From classical to quantum. **Rev. Mod. Phys.**, American Physical Society, v. 93, p. 035008, Sep 2021. Disponível em: <https://link.aps.org/doi/10.1103/RevModPhys.93.035008>. Cited 2 times on pages 29 e 30

[35] ASSIS, R. J. de et al. Efficiency of a quantum otto heat engine operating under a reservoir at effective negative temperatures. **Phys. Rev. Lett.**, American Physical Society, v. 122, p. 240602, Jun 2019. Disponível em: <https://link.aps.org/doi/10.1103/PhysRevLett.122.240602>. Cited 2 times on pages 32 e 35

[36] OLIVEIRA, I. S. **NMR Quantum Information Processing**. [S.l.]: Elsevier, 2007. Cited 3 times on pages 62, 63 e 65

[37] LEVITT, M. **Spin Dynamics: Basics of nuclear magnetic resonance**. [S.l.]: John Wiley Sons Ltd, 2012. Cited 2 times on pages 65 e 66

APPENDICES

APPENDIX A

Master Equation for a Fermionic Reservoir

To obtain the Markovian master equation considering a fermionic reservoir, let's assume that the Hamiltonian describing the reservoir is given by

$$H_R = \frac{\hbar}{2}\sum_j \omega_j \sigma_{z,j}, \tag{A.1}$$

The reservoir state is described by a Gibbs state

$$\rho_R(0) = \prod_j \frac{e^{-\beta\hbar\omega_{z,j}}}{e^{\beta\hbar\omega_{z,j}} + e^{-\beta\hbar\omega_{z,j}}}, \tag{A.2}$$

and the Hamiltonian that describes the system is

$$H_S = \frac{\hbar}{2}\omega_0\sigma_z. \tag{A.3}$$

Now, in order to derive the Markovian master equation, we need to consider the interaction between the system and the reservoir. This interaction can be described by the Hamiltonian

$$H_I = \hbar\sum(\kappa_j^*\sigma_-\sigma_{+,j} + \kappa_j\sigma_+\sigma_{-,j}), \tag{A.4}$$

where $s_1 = \sigma_-$ and $s_2 = \sigma_+$, $R_1 = \sum_j \kappa_j^*\sigma_{+,j}$ and $R_2 = \sum_j \kappa_j\sigma_{-,j}$. Transitioning to the interaction representation, we obtain that

$$\tilde{s}_1 = \sigma_- e^{-i\omega_0 t} \tag{A.5}$$

$$\tilde{s}_2 = \sigma_+ e^{i\omega_0 t} \tag{A.6}$$

$$\tilde{R}_1 = \sum_j \kappa_j^*\sigma_{+,j}e^{i\omega_j t} \tag{A.7}$$

$$\tilde{R}_2 = \sum_j \kappa_j \sigma_{-,j} e^{-i\omega_j t}. \tag{A.8}$$

So, the master equation becomes

$$\begin{aligned}
\dot{\tilde{\rho}}_S(t) = -\int_0^t dt' \Big\{ & [\sigma_-\sigma_-\tilde{\rho}_S(t) - \sigma_-\tilde{\rho}_S(t)\sigma_-] e^{-i\omega_0(t+t')} \left\langle \tilde{R}_1(t)\tilde{R}_1(t') \right\rangle_R + \text{h.c} \\
& - [\tilde{\rho}_S(t)\sigma_-\sigma_- - \sigma_-\tilde{\rho}_S(t)\sigma_-] e^{-i\omega_0(t+t')} \left\langle \tilde{R}_1(t')\tilde{R}_1(t) \right\rangle_R + \text{h.c} \\
& - [\sigma_-\sigma_+\tilde{\rho}_S(t) - \sigma_+\tilde{\rho}_S(t)\sigma_-] e^{-i\omega_0(t-t')} \left\langle \tilde{R}_1(t)\tilde{R}_2(t') \right\rangle_R + \text{h.c} \\
& - [\tilde{\rho}_S(t)\sigma_+\sigma_- - \sigma_-\tilde{\rho}_S(t)\sigma_+] e^{-i\omega_0(t-t')} \left\langle \tilde{R}_2(t')\tilde{R}_1(t) \right\rangle_R + \text{h.c} \Big\}.
\end{aligned} \tag{A.9}$$

Reservoir correlation functions can be expressed as:

$$\begin{aligned}
\left\langle \tilde{R}_2(t)\tilde{R}_2(t') \right\rangle_R &= \sum_{i,j} \kappa_j^* \kappa_k^* e^{i\omega_j t} e^{i\omega_k t'} \operatorname{tr}_R \{\sigma_{+,j}\sigma_{+,k}\rho_R(0)\} \\
\left\langle \tilde{R}_2(t')\tilde{R}_2(t) \right\rangle_R &= \sum_{i,j} \kappa_j^* \kappa_k^* e^{i\omega_j t'} e^{i\omega_k t} t_R \{\sigma_{+,j}\sigma_{+,k}\rho_R(0)\} \\
\left\langle \tilde{R}_2(t)\tilde{R}_1(t') \right\rangle_R &= \sum_{i,j} \kappa_j^* \kappa_k e^{i\omega_j t} e^{-i\omega_k t'} \operatorname{tr}_R \{\sigma_{+,j}\sigma_{-,k}\rho_R(0)\} \\
\left\langle \tilde{R}_1(t')\tilde{R}_2(t) \right\rangle_R &= \sum_{i,j} \kappa_j \kappa_k^* e^{-i\omega_j t'} e^{i\omega_k t} \operatorname{tr}_R \{\sigma_{-,j}\sigma_{+,k}\rho_R(0)\} \\
\left\langle \tilde{R}_1(t)\tilde{R}_2(t') \right\rangle_R &= \sum_{i,j} \kappa_j \kappa_k^* e^{-i\omega_j t} e^{i\omega_k t'} \operatorname{tr}_R \{\sigma_{-,j}\sigma_{+,k}\rho_R(0)\} \\
\left\langle \tilde{R}_2(t')\tilde{R}_1(t) \right\rangle_R &= \sum_{i,j} \kappa_j^* \kappa_k e^{i\omega_j t'} e^{-i\omega_k t} \operatorname{tr}_R \{\sigma_{+,j}\sigma_{-,k}\rho_R(0)\} \\
\left\langle \tilde{R}_1(t)\tilde{R}_1(t') \right\rangle_R &= \sum_{i,j} \kappa_j \kappa_k e^{-i\omega_j t} e^{-i\omega_k t'} \operatorname{tr}_R \{\sigma_{-,j}\sigma_{-,k}\rho_R(0)\} \\
\left\langle \tilde{R}_1(t')\tilde{R}_1(t) \right\rangle_R &= \sum_{i,j} \kappa_j \kappa_k e^{-i\omega_j t'} e^{-i\omega_k t} \operatorname{tr}_R \{\sigma_{-,j}\sigma_{-,k}\rho_R(0)\}.
\end{aligned} \tag{A.10}$$

Note that in the case where $j = k$, we have $\operatorname{tr} R(\sigma\pm, j\sigma_{\pm,k}\rho_R(0)) = 0$, given that $\sigma_{\pm,j}\sigma_{\pm,j} = 0$. Now, considering the scenario where $j \neq k$,

$$\begin{aligned}
\operatorname{tr}_R \left(\sigma_{\pm,j}\sigma_{\pm,k}\rho_R(0)\right)_{j\neq k} &= \operatorname{tr}_R \left[\sigma_{\pm,j}\sigma_{\pm,k} \prod_l \frac{e^{-\beta\hbar/2\omega_l\sigma_{z,l}}}{e^{\beta\hbar/2\omega_l} + e^{-\beta\hbar/2\omega_l}}\right] \\
&= \left\{\frac{\operatorname{tr}_{R_j}\left[\sigma_{\pm,j}e^{-\beta\hbar/2\omega_j\sigma_{z,j}}\right]}{e^{\beta\hbar/2\omega_j} + e^{-\beta\hbar/2\omega_j}}\right\} \left\{\frac{\operatorname{tr}_{R_k}\left[\sigma_{\pm,k}e^{-\beta\hbar/2\omega_k\sigma_{z,k}}\right]}{e^{\beta\hbar/2\omega_k} + e^{-\beta\hbar/2\omega_k}}\right\} \\
&= 0.
\end{aligned} \tag{A.11}$$

Similarly, we have $\mathrm{tr}\, R\left(\sigma\pm, j\sigma_{\mp,k}\rho_R(0)\right) = 0$. See below:

$$\begin{aligned}\mathrm{tr}_R\left(\sigma_{\pm,j}\sigma_{\mp,k}\rho_R(0)\right)_{j\neq k} &= \mathrm{tr}_R\left[\sigma_{\pm,j}\sigma_{\mp,k}\prod_l \frac{e^{-\beta\hbar/2\omega_l\sigma_{z,l}}}{e^{\beta\hbar/2\omega_l}+e^{-\beta\hbar/2\omega_l}}\right]\\ &= \left\{\frac{\mathrm{tr}_{R_j}\left[\sigma_{\pm,j}e^{-\beta\hbar/2\omega_j\sigma_{z,j}}\right]}{e^{\beta\hbar/2\omega_j}+e^{-\beta\hbar/2\omega_j}}\right\}\left\{\frac{\mathrm{tr}_{R_k}\left[\sigma_{\mp,k}e^{-\beta\hbar/2\omega_k\sigma_{z,k}}\right]}{e^{\beta\hbar/2\omega_k}+e^{-\beta\hbar/2\omega_k}}\right\}\\ &= 0.\end{aligned} \tag{A.12}$$

In the scenario where $j = k$, it is essential to compute the traces separately, as demonstrated below:

$$\begin{aligned}\mathrm{tr}_R\left(\sigma_{+,j}\sigma_{-,j}\rho_R(0)\right) &= \mathrm{tr}_R\left[\sigma_{+,j}\sigma_{-,j}\prod_l \frac{e^{-\beta\hbar/2\omega_l\sigma_{z,l}}}{e^{\beta\hbar/2\omega_l}+e^{-\beta\hbar/2\omega_l}}\right]\\ &= \frac{\mathrm{tr}_{R_j}\left[\sigma_{+,j}\sigma_{-,j}e^{-\beta\hbar/2\omega_j\sigma_{z,j}}\right]}{e^{\beta\hbar/2\omega_j}+e^{-\beta\hbar/2\omega_j}}\\ &= \frac{\left\langle g_j\left|\sigma_{+,j}\sigma_{-,j}e^{-\beta\hbar/2\omega_j\sigma_{z,j}}\right|g_j\right\rangle + \left\langle e_j\left|\sigma_{+,j}\sigma_{-,j}e^{-\beta\hbar/2\omega_j\sigma_{z,j}}\right|e_j\right\rangle}{e^{\beta\hbar/2\omega_j}+e^{-\beta\hbar/2\omega_j}}\\ &= \frac{\left\langle g_j\left|\sigma_{+,j}\sigma_{-,j}\right|g_j\right\rangle e^{\beta\hbar/2\omega_j\sigma_{z,j}} + \left\langle e_j\left|\sigma_{+,j}\sigma_{-,j}\right|e_j\right\rangle e^{-\beta\hbar/2\omega_j\sigma_{z,j}}}{e^{\beta\hbar/2\omega_j}+e^{-\beta\hbar/2\omega_j}}\\ &= \frac{e^{-\beta\hbar/2\omega_j}}{e^{\beta\hbar/2\omega_j}+e^{-\beta\hbar/2\omega_j}}\\ &= \frac{1}{e^{\beta\hbar\omega_j}+1}\\ &= \bar{n}_f\left(\omega_j,\beta\right).\end{aligned}$$

In this context, $\bar{n}_f\left(\omega j,\beta\right)$ denotes the average number of electrons occupying the excited state of atom j, in accordance with the Fermi-Dirac distribution. Finally,

$$\begin{aligned}\mathrm{tr}_R\left(\sigma_{-,j}\sigma_{+,j}\rho_R(0)\right) &= \mathrm{tr}_R\left[\left(1-\sigma_{-,j}\sigma_{+,j}\rho_R(0)\right)\rho_R(0)\right]\\ &= 1-\bar{n}_f\left(\omega_j,\beta\right).\end{aligned} \tag{A.13}$$

In summary, the results are

$$\begin{aligned}\mathrm{tr}_R\left\{\sigma_{+,j}\sigma_{-,k}\rho_R(0)\right\} &= \bar{n}_f\left(\omega_j,\beta\right)\delta_{j,k}\\ \mathrm{tr}_R\left\{\sigma_{-,j}\sigma_{+,k}\rho_R(0)\right\} &= \left[1-\bar{n}_f\left(\omega_j,\beta\right)\delta_{j,k}\right]\\ \mathrm{tr}_R\left\{\sigma_{\pm,j}\sigma_{\pm,k}\rho_R(0)\right\} &= 0.\end{aligned}$$

Thus, Equation A.10 becomes

$$\begin{aligned}
\left\langle \tilde{R}_2(t)\tilde{R}_1\left(t'\right)\right\rangle_R &= \sum_j \left|\kappa_j\right|^2 e^{i\omega_j(t-t')}\bar{n}_f\left(\omega_j,\beta\right), \\
\left\langle \tilde{R}_1\left(t'\right)\tilde{R}_2(t)\right\rangle_R &= \sum_j \left|\kappa_j\right|^2 e^{i\omega_j(t-t')}\left[1-\bar{n}_f\left(\omega_j,\beta\right)\right], \\
\left\langle \tilde{R}_1(t)\tilde{R}_2\left(t'\right)\right\rangle_R &= \sum_j \left|\kappa_j\right|^2 e^{-i\omega_j(t-t')}\left[1-\bar{n}_f\left(\omega_j,\beta\right)\right], \\
\left\langle \tilde{R}_2\left(t'\right)\tilde{R}_1(t)\right\rangle_R &= \sum_j \left|\kappa_j\right|^2 e^{-i\omega_j(t-t')}\bar{n}_f\left(\omega_j,\beta\right).
\end{aligned} \tag{A.14}$$

Therefore, the master equation reduces to

$$\begin{aligned}
\frac{d\tilde{\rho}(t)}{dt} = -\int_0^t dt' \Big\{ &\left[\sigma_-\sigma_+\tilde{\rho}\left(t'\right) - \sigma_+\tilde{\rho}\left(t'\right)\sigma_-\right] e^{-i\omega_0(t-t')}\left\langle \tilde{R}_2(t)\tilde{R}_1\left(t'\right)\right\rangle_R \\
&+ \left[\tilde{\rho}\left(t'\right)\sigma_+\sigma_- - \sigma_-\tilde{\rho}\left(t'\right)\sigma_+\right] e^{-i\omega_0(t-t')}\left\langle \tilde{R}_1\left(t'\right)\tilde{R}_2(t)\right\rangle_R \\
&+ \left[\sigma_+\sigma_-\tilde{\rho}\left(t'\right) - \sigma_-\tilde{\rho}\left(t'\right)\sigma_+\right] e^{i\omega_0(t-t')}\left\langle \tilde{R}_1(t)\tilde{R}_2\left(t'\right)\right\rangle_R \\
&+ \left[\tilde{\rho}\left(t'\right)\sigma_-\sigma_+ - \sigma_+\tilde{\rho}\left(t'\right)\sigma_-\right] e^{i\omega_0(t-t')}\left\langle \tilde{R}_2\left(t'\right)\tilde{R}_1(t)\right\rangle_R .
\end{aligned} \tag{A.15}$$

Now, applying the same approximations and considerations as in Equations 3.39 to 3.46, we obtain the master equation for fermionic reservoirs.

$$\begin{aligned}
\frac{d\tilde{\rho}(t)}{dt} = -i\omega_A\left[\sigma_+\sigma_-,\tilde{\rho}(t)\right] &+ \frac{\gamma}{2}(1-\bar{n}_f)\left[2\sigma_-\tilde{\rho}(t)\sigma_+ - \sigma_+\sigma_-\tilde{\rho}(t) - \tilde{\rho}(t)\sigma_+\sigma_-\right] \\
&+ \frac{\gamma}{2}\bar{n}_f\left[2\sigma_+\tilde{\rho}(t)\sigma_- - \sigma_-\sigma_+\tilde{\rho}(t) - \tilde{\rho}(t)\sigma_-\sigma_+\right].
\end{aligned}$$

APPENDIX B

Nuclear Magnetic Resonance concepts

The NMR technique utilizes a fixed magnetic field and radio frequency (RF) pulses to manipulate the behavior of nuclear spins. This spectrometer allows for the analysis and preparation of the quantum state of a given system, execution of logical operations, and the implementation of quantum algorithms through unitary transformations.

B.1 General Concepts

The systems of interest are magnetic systems with angular momentum, such as electrons and atomic nuclei. In NMR, nuclei are treated as quantum entities, while magnetic fields are approached in a classical way. Thus, the semiclassical description of the interaction between an atomic nucleus and a magnetic field is expressed through a Hamiltonian:

$$H = \vec{\mu} \cdot \vec{B}, \tag{B.1}$$

where $\vec{\mu}$ is the magnetic dipole moment vector operator and $\vec{B}$ is the magnetic field vector. The magnetic dipole moment can be expressed as

$$\mu = \gamma_n \vec{I}, \tag{B.2}$$

in this context, γ_n represents the nuclear gyromagnetic factor (a constant unique to each atomic nucleus), and $\vec{I}$ is the nuclear spin operator, symbolizing the total angular momentum of the nucleus.

The states commonly used to expand the nuclear spin operator and therefore the

Hamiltonian H are denoted by the states $|I, m_i\rangle$. These states satisfy the relations:

$$\hat{I}^2|I, m_i\rangle = I(I+1)|I, m_i\rangle \tag{B.3}$$

and

$$\hat{I}_z|I, m_i\rangle = m_i|I, m_i\rangle, \tag{B.4}$$

where $\hat{I}_z$ is the z component of the spin operator $\hat{I}$ and I is the nuclear spin quantum number. For each value of I, which can be an integer or half-integer, there is a subspace with $2I+1$ states $|I, m_i\rangle$, corresponding to $m_i = -I, -I+1, \ldots, I-1, I$. The operators that promote transitions between states $|I, m_i\rangle$ are the lifting and lowering operators, represented here by I_+ and I_-, respectively. The action of these operators on the states $|I, m_i\rangle$ results in:

$$I_+|I, m_i\rangle = \sqrt{I(I+1) - m_i(m_i+1)}|I, m_i+1\rangle \tag{B.5}$$

and

$$I_-|I, m_i\rangle = \sqrt{I(I+1) - m_i(m_i-1)}|I, m_i-1\rangle. \tag{B.6}$$

Specifically, the raising and lowering operators are given by $I_+ = I_x + iI_y$ and $I_- = I_x - iI_y$, where I_x and I_y are the x and y components of the nuclear spin operator.

Considering that there are no transitions between states with different quantum numbers I, we can affirm that the nuclear spin is constant [36]. Thus, the quantum number I defines the subspace in which transitions occur, given by $\{|I, -I\rangle, |I, -I+1\rangle, \ldots, |I, I-1\rangle, |I, I\rangle\}$. For atomic nuclei with $I = 1/2$, such as in the case of hydrogen nuclei ^{1}H and carbon nuclei ^{13}C, transitions occur between the states $|1/2, -1/2\rangle$ and $|1/2, 1/2\rangle$.

B.2 The interaction of the atomic nucleus with static fields

When subjecting an atomic nucleus, which possesses intrinsic magnetic moments, to a static magnetic field B_0 (external to the nucleus), the nuclear states $|I, m_i\rangle$ will assume different energy values. These energy values depend on the orientation of the nuclear spin concerning the magnetic field. This interaction causes a breaking of degeneracy among the energy levels of the nuclear spin

$$H_L = -\vec{\mu} \cdot \vec{B}_0, \tag{B.7}$$

Considering that the static magnetic field, B_0, is aligned in the direction z, and

taking into consideration the particular case of a nucleus with *spin* $\frac{1}{2}$,

$$\vec{\mu} = \frac{1}{2}\hbar\gamma_n(\sigma_x\hat{x} + \sigma_y\hat{y} + \sigma_z\hat{z}) \tag{B.8}$$

the Equation B.7 can be rewritten as:

$$H_L = -\frac{1}{2}\hbar\omega_L\sigma_z \tag{B.9}$$

The Larmor frequency, represented by ω_L, is defined as $\omega_L = \gamma_n B_0$. As mentioned earlier, γ_n refers to the nuclear gyromagnetic ratio, while B_0 represents the magnitude of the applied static magnetic field. This frequency indicates the rate at which nuclear spins precess in response to the external magnetic field.

Therefore, for a transition between the energy eigenstates of the Hamiltonian $H_L(|1/2, 1/2\rangle, |1/2, -1/2\rangle)$ to occur, the nuclear spin must absorb or release an amount of energy equal to $\Delta E = \hbar\omega_L$.

Heteronuclear molecules, such as chloroform, exhibit a significant disparity in the precession frequencies of ^1H and ^{13}C spins [36]. This difference facilitates the individual manipulation of each of the nuclei present in the molecule.

B.3 Radiofrequency Field

Assuming that the degeneracy of energy levels has been broken by a static magnetic field, the magnetic field capable of inducing transitions between the ground states $|-\rangle$ and excited states $|+\rangle$ of the nucleus must oscillate approximately at the Larmor frequency, where $\Delta E = E_+ - E_- = \hbar\omega_L$. Magnetic resonance frequencies (Larmor frequencies) typically fall in the radiofrequency region (for nuclear spins).

Using the time-dependent perturbation theory, the transition probability from the state $|-\rangle$ to the state $|+\rangle$ is described by the following expression:

$$P_{|-\rangle\to|+\rangle} = \frac{1}{\hbar^2}\left|\int_0^t dt' \mathrm{e}^{i\omega_L t'} \langle + |H_{RF}(t')| - \rangle\right|^2, \tag{B.10}$$

being $H_{RF}(t) = -\vec{\mu}\cdot\vec{B}_{RF}(t)$, with $\vec{B}_{RF}(t)$ being the radiofrequency magnetic field. Considering circular polarization in the xy plane, the radiofrequency magnetic field is given by:

$$\vec{B}_{RF}(t) = B_{RF}\left[\cos(\omega_{RF}t + \phi)\,\hat{x} + \mathrm{sen}\,(\omega_{RF}t + \phi)\,\hat{y}\right], \tag{B.11}$$

where B_{RF} is the amplitude of the field, ω_{RF} is the frequency at which it oscillates, and ϕ is the phase. Thus, the resonant interaction between the atomic nucleus and the

radiofrequency magnetic field is then described by the Hamiltonian:

$$H_{RF}(t) = -\frac{1}{2}\hbar\Omega_{RF}\left[\cos\left(\omega_L t + \phi\right)\sigma_x + \sin\left(\omega_L t + \phi\right)\sigma_y\right] \tag{B.12}$$

in which $\Omega_{RF} = \gamma_n B_{RF}$.

In the presence of the static magnetic field and the radiofrequency magnetic field, the dynamics of an ensemble of atoms with $I = 1/2$ is described by the von Neumann equation. The total Hamiltonian consists of two parts, where $H(t) = H_L + H_{RF}(t)$.

Making a change to the interaction representation and applying the operators $U_0(t) = \mathrm{e}^{-iH_0 t/\hbar} = \mathrm{e}^{-iH_L t/\hbar}$ and $U_0^\dagger(t)$, we obtain the von Neumann equation in the interaction representation.

$$\frac{d\tilde{\rho}(t)}{dt} = \frac{1}{i\hbar}[\tilde{H}(t), \tilde{\rho}(t)]$$

with

$$\tilde{H}(t) = U_0^\dagger(t) H_{RF}(t) U_0(t)$$

and

$$\tilde{\rho}(t) = U_0^\dagger(t)\rho(t)U_0(t)$$

it can be observed that the Hamiltonian in the interaction representation is explicitly given by the expression:

$$\tilde{H} = -\frac{1}{2}\hbar\Omega_{RF}\left[\cos(\phi)\sigma_x + \mathrm{sen}(\phi)\sigma_y\right] \tag{B.13}$$

The initial state of the NMR experiment involving an ensemble of atomic nuclei with $I = 1/2$ is given by the Gibbs state

$$\rho_G = \frac{e^{-\beta H_L}}{Z}, \tag{B.14}$$

considering that in the limits of high temperatures, i.e., $\beta\hbar\omega_L << 1$, we then have

$$\rho_G = \frac{1}{2}\left(\mathrm{I} + \frac{1}{2}\beta\hbar\omega_L\sigma_z\right), \tag{B.15}$$

when applying the temporal evolution operator $U(t) = \mathrm{e}^{-i\tilde{H}t/\hbar}$ and $U^\dagger(t)$ to the left and right of the equation B.15, one obtains:

$$\tilde{\rho}(t) = \frac{1}{2}\left[\mathcal{I} + \frac{1}{2}\beta\hbar\omega_L U(t)\sigma_z U^\dagger(t)\right], \tag{B.16}$$

note that only the part of the state ρ_G containing σ_z undergoes the action of the radiofrequency magnetic field.

The order of magnitude of frequencies used in NMR experiments shows that

Equation B.16 is not capable of fully describing the dynamics of pure states [36]. However, it is possible to achieve this description by considering only the part of the state affected by $\vec{B}_{RF}(t)$. The idea, considering the example of a pure state, is to find a set of operations that transforms the state ρ_G into the state:

$$\tilde{\rho}_{|\psi\rangle} = \frac{1}{2}(1-\epsilon)\mathcal{I} + \epsilon|\tilde{\psi}\rangle\langle\tilde{\psi}|, \tag{B.17}$$

where ϵ a constant and $|\tilde{\psi}\rangle$ the desired pure state, which is called a pseudo-pure state. Thus, the temporal evolution of $\tilde{\rho}_{|\psi\rangle}$ is given by:

$$\tilde{\rho}_{|\psi\rangle} = \frac{1}{2}(1-\epsilon)\mathcal{I} + \epsilon U(t)|\tilde{\psi}\rangle\langle\tilde{\psi}|U^{\dagger}(t), \tag{B.18}$$

therefore, the quantum dynamics of the pseudo-pure state become evident. From the pseudo-pure state, it is possible to construct any other state.

B.4 Relaxation Processes

When applying radiofrequency pulses in a transverse plane, nuclear spins, due to the presence of the static magnetic field B_0, precess around the z-axis, resulting in a non-equilibrium configuration. After a characteristic time, magnetization returns along the z-axis, recovering its equilibrium value in the rotating frame. This phenomenon is known as nuclear spin relaxation, involving simultaneous and independent processes of transverse relaxation and longitudinal relaxation, each with characteristic times.

The longitudinal relaxation time T_1 corresponds to the characteristic time associated with the recovery of magnetization in the direction of the static magnetic field (z-axis) after being disturbed by a radiofrequency pulse. On the other hand, the transverse relaxation time T_2 corresponds to the characteristic time associated with the loss of phase coherence among nuclear spins in the transverse plane, resulting in the decrease of the transverse component of magnetization [37]. The relaxation processes can be described through the Bloch equations:

$$\frac{dM_z}{dt} = \frac{M_0 - M_z}{T_1}, \tag{B.19}$$

$$\frac{dM_{xy}}{dt} = -\frac{M_{xy}}{T_2}. \tag{B.20}$$

We can express the evolution of the transverse and longitudinal magnetization components as follows:

$$M_{x,y} = M_0 e^{-\frac{t}{T_2}}, \tag{B.21}$$

and

$$M_z = M_0\left(1 - e^{-\frac{t}{T_1}}\right). \tag{B.22}$$

The relaxation time T_1 is associated with the return of equilibrium magnetization and determines the interval between consecutive experiments. On the other hand, T_2 is linked to the loss of coherence in the transverse component of magnetization, influencing the complexity of logical gate sequences in quantum information experiments [37] . Both are fundamental for understanding and controlling processes in quantum systems under NMR.